

Outage Probability Region and Optimal Power Allocation for Uplink SCMA Systems

Jiaxuan Chen, Zhaocheng Wang[✉], *Senior Member, IEEE*, Wei Xiang[✉], *Senior Member, IEEE*,
and Sheng Chen[✉], *Fellow, IEEE*

Abstract—As a promising non-orthogonal multiple access scheme, sparse code multiple access (SCMA) technology has attracted much attention. Because inter-user interference is present in code domain and multi-user iterative detection is required, user capacity and outage probability analysis for uplink SCMA systems are challenging and have not been presented in the literature. In this paper, the capacity region for uplink SCMA systems is analyzed, based on which the common and individual outage probability regions are calculated. Optimizing the outage probability within the outage probability region can be casted as an Lagrangian duality problem and solved by an iterative descent algorithm, which however imposes high complexity since the expectation operation is required in each iteration. To reduce the computational complexity of solving this Lagrangian duality problem, an adaptive algorithm is developed, which is capable of providing the optimal outage probability and adaptively updating it. Furthermore, a power allocation policy is naturally obtained to achieve the optimized outage probability in the outage probability region.

Index Terms—Sparse code multiple access, capacity region, common outage probability region, individual outage probability region, power allocation policy.

I. INTRODUCTION

IN RECENT time, the fifth generation (5G) technology emerges to support massive connectivity, high throughput, and low latency demands of the next generation mobile network [1], [2]. In particular, massive connectivity is one of the main user requirements for 5G systems, because in these future mobile networks, cell sizes become very small and access points become extremely dense. Non-orthogonal

multiple access (NOMA) is a promising candidate approach to support massive connectivity by allowing controllable inter-user interference (IUI) [3].

Sparse code multiple access (SCMA) is a class of NOMA schemes supporting more number of users than its orthogonal counterparts by introducing interference in the code domain [4]–[6]. Code division multiple access (CDMA) technology is a mature code domain multiple access scheme, whereby a unique spreading sequence is allocated to each user [7], [8]. However, when massive connectivity is required, and the number of users is larger than that of orthogonal code resources, it is impossible to maintain orthogonality among the spread sequences [9]. Multi-user detection is an efficient method to deal with IUI, which however imposes a comparatively high complexity. The low density signature (LDS) scheme strikes a trade-off between decoding complexity and robustness against IUI, where a sparse indicator matrix is designed as the spread sequences, and the message passing algorithm (MPA) is employed to reduce the decoding complexity [10], [11]. Since the non-zero elements of CDMA (or LDS) codewords are derived from multiplying the same symbol by different chips in the spread sequences, the shaping gain of the multi-dimensional resource is not fully utilized.

The codebook for SCMA, however, directly maps information bits onto well-designed multi-dimensional constellations rather than utilizing spread sequences like LDS. Owing to its well-designed multi-dimensional constellations, SCMA is able to realize the shaping gain and to outperform its LDS counterpart [4]. Various methods have been proposed to design SCMA codebooks. The work [12] proposed a general codebook design process, which consists of two components, mother constellation and constellation operation design. A star-QAM based codebook was proposed in [13] to increase the minimum Euclidean distance of the mother constellation. In [14], the constellation design was combined with resource allocation to enhance the bit error rate (BER) performance. An irregular codebook design was proposed in [15] to satisfy different demands of different users. Several decoding algorithms were also discussed to improve the decoding speed and accuracy [16]–[19]. Some theoretical analysis for the performance of SCMA systems have also been carried out. For example, the work [20] provided the error probability bounds by simplifying an SCMA system to a single-user single-input and multiple-output model.

Manuscript received December 5, 2017; revised March 29, 2018 and May 28, 2018; accepted May 28, 2018. Date of publication June 4, 2018; date of current version October 16, 2018. This work was supported in part by National Natural Science Foundation of China under Grant 61571267, in part by Shenzhen Subject Arrangements (JCYJ20160331184124954), and in part by Shenzhen Fundamental Research Project (JCYJ20170307153116785). The associate editor coordinating the review of this paper and approving it for publication was V. Raghavan. (*Corresponding author: Zhaocheng Wang.*)

J. Chen and Z. Wang are with the Beijing National Research Center for Information Science and Technology, Department of Electronic Engineering, Tsinghua University, Beijing 100084, China (e-mail: chenjx16@mails.tsinghua.edu.cn; zcwang@tsinghua.edu.cn).

W. Xiang is with the College of Science and Engineering, James Cook University, Cairns QLD 4878, Australia (e-mail: wei.xiang@jcu.edu.au).

S. Chen is with the School of Electronics and Computer Science, University of Southampton, Southampton SO17 1BJ, U.K., and also with King Abdulaziz University, Jeddah 21589, Saudi Arabia (e-mail: sqc@ecs.soton.ac.uk).

Color versions of one or more of the figures in this paper are available online at <http://ieeexplore.ieee.org>.

Digital Object Identifier 10.1109/TCOMM.2018.2843354

In [21], receiver diversity and users' position variance were considered in the symbol error rate analysis.

It is well understood that capacity and throughput are important performance metrics. For power-domain NOMA (PD-NOMA) schemes, a closed-form capacity expression can be derived due to the simple successive decoding algorithm used [22]–[24]. Unfortunately, unlike PD-NOMA systems, it is difficult to obtain an explicit capacity expression for the users in uplink SCMA systems. This is because iterative multi-user detection instead of successive signal detections is required for SCMA uplink, and the interactions among the multi-dimensional signals for different users also make the theoretical analysis challenging. The sum capacity of all the users in SCMA systems was analyzed in [25], but individual user's capacity were not considered. The works [26] and [27] studied how to assign all the possible sparse codebooks among the system's users, but the interactions among the different users in a cell were not considered and these two works did not analyze individual user's capacity. The study [28] investigated the cutoff capacity of SCMA systems. However, only downlink broadcast scenario was considered, where the signals for different users go through the same channel. For uplink SCMA systems, the achievable data rate of each individual user and how the interactions among different users influences the achievable data rates of individual users have not been analyzed. Thus the outage probability has not been provided in the existing literature for uplink SCMA systems.

Since the capacity and outage probability are important metrics for uplink SCMA systems, in this paper, we first derive the capacity region of uplink SCMA systems based on the capacity region theory of multiple access channels (MACs) [29], where a data rate vector in the capacity region represents an achievable combination of the data rates for all the users. With the aid of this expression of the SCMA capacity region, we exploit the interactions among all the users to derive the common outage probability region and individual outage probability region [30] given a required data rate vector, which describes the common system performance and each individual user's performance, respectively. Then the optimization of the outage probability within the outage probability region can be casted as an Lagrangian duality problem and solved by an iterative descent algorithm. However, the expectation operation is required in each iteration and in the calculation of the outage probability, which imposes high complexity. To reduce the computational complexity, the outage probability optimization problem is reformulated, and an adaptive algorithm that does not need expectation operation is proposed to obtain the optimal outage probability and to adaptively update it. During the optimization process, an optimal power allocation scheme is naturally obtained to achieve the desired outage probability. In the simulation study, the SCMA capacity region and outage probability region are evaluated. We also demonstrate that the proposed power allocation algorithm works well for practical uplink SCMA systems. The main contributions of this paper are summarized as follows.

- For the first time, the capacity region of the uplink SCMA system is derived, which considers the characteristics of

the multi-dimensional constellation as well as highlights the interactions among all the user.

- Based on the expression of the capacity region, the common and individual outage probability regions are analyzed for the first time, which provides a useful tool to evaluate the performance of SCMA systems given the power constraint. The optimization of the outage probability in the outage probability region is transformed into an Lagrangian dual problem, which can be solved by the iterative descent method.
- To reduce the computational complexity, the outage probability optimization is reformulated and an adaptive algorithm is proposed to update the optimal outage probability adaptively. Moreover, an optimal power allocation policy is naturally obtained to achieve the desired outage probability.

The remainder of this paper is structured as follows. Section II briefly introduces the uplink SCMA system model and the characteristics of SCMA codebooks. Section III derives the expression of the SCMA capacity region and compares it with that of CDMA. Section IV introduces the common outage probability region and formulates the problem of minimizing the common outage probability given certain power constraint. In section V, an adaptive algorithm is proposed to optimize the common outage probability with low complexity, which leads to a corresponding power allocation policy. The adaptive algorithm is also applied to the individual outage probability region in Section VI. Section VII presents simulation results, where the capacity region and outage probability region are evaluated and the performance of the proposed adaptive algorithm is investigated. We also show that the proposed power allocation algorithm works well for practical uplink SCMA systems. Section VIII briefly describes how to extend our approach to multi-cell uplink SCMA. Our concluding remarks are drawn in section IX.

We adopt the following notation conventions. For $\mathbf{v} \in \mathbb{C}^K$, v_i is its i th element for $1 \leq i \leq K$, and the elements of $\mathbf{F} \in \mathbb{C}^{K \times M}$ are denoted by $f_{i,j}$ for $1 \leq i \leq K$ and $1 \leq j \leq M$, while $\text{diag}(\mathbf{v})$ or $\text{diag}(v_1, v_2, \dots, v_K)$ denotes the $K \times K$ diagonal matrix whose diagonal elements are v_1, v_2, \dots, v_K . The transpose and conjugate transpose operators are denoted by $(\cdot)^T$ and $(\cdot)^H$, respectively, while $\mathbf{1}_K$ is the K -dimensional vector with all the elements equal to 1, \mathbf{I}_K is the $K \times K$ identity matrix and $\mathbf{0}$ denotes the zero matrix or vector of appropriate dimension. The expectation operator is denoted by $E\{\cdot\}$, and $\det(\cdot)$ denotes the matrix determinant operation, while $j = \sqrt{-1}$. For $v \in \mathbb{C}$, $|v|$ is the magnitude of v , and for matrix \mathbf{V} , $|\mathbf{V}|$ is the matrix obtained by replacing every element of \mathbf{V} with its magnitude, while for set \mathcal{S} , $|\mathcal{S}|$ is the cardinality of \mathcal{S} . The probability of event \mathcal{A} is denoted by $\Pr[\mathcal{A}]$, and the superscript $*$ denotes the optimal solution of an optimization problem. The truncation $(\mathbf{x})_\varepsilon^+$ of real vector \mathbf{x} is element-wise as: $(x_i)_\varepsilon^+ = x_i$ if $x_i > \varepsilon$ and otherwise $(x_i)_\varepsilon^+ = \varepsilon$, $\forall i$. Inequality for same-size vectors is defined element-wise as: $\mathbf{a} \leq \mathbf{b}$ means $a_i \leq b_i$, $\forall i$. $\|\cdot\|$ is the vector/matrix two norm, and the dot product operator \odot of two same-size vectors or matrices is defined element-wise.

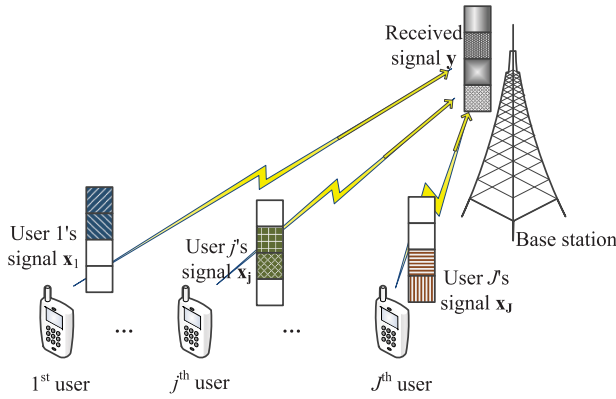


Fig. 1. Codeword structure of an uplink SCMA system, where the BS of each cell employs K orthogonal resources to serve J users, and the non-orthogonal sharing of the K orthogonal resources among the users is allowed.

II. SYSTEM MODEL

As illustrated in Fig. 1, an uplink SCMA system is considered, where the base station (BS) of each cell employs K orthogonal resources to serve J users,¹ and the non-orthogonal sharing of the K orthogonal resources among the users is allowed [4], [12]. For user j , the encoder first maps $N_{B,j}$ information bits onto an N_j -dimensional code or symbol vector c_j , which is selected from the unique constellation alphabet \mathcal{C}_j for the j th user. Next c_j is spread to a sparse K -dimensional transmit signal vector x_j by padding zeros. The positions of zeros for the users' transmit signal vectors x_j are represented by an $K \times J$ resource assignment matrix \mathbf{F} [12]. Specifically, the indices of zeros in the j th column of \mathbf{F} indicate the indices of the zeros in the j th user's transmit signal vector x_j , whereas the indices of the ones in the j th column imply that the corresponding resources are utilized by the j th user. In this way, \mathbf{F} completely specifies the users' transmit signal vectors x_j from c_j for $1 \leq j \leq J$. Therefore, the design of \mathbf{F} is also called codebook assignment [31]. \mathbf{F} and $\{\mathcal{C}_j\}_{j=1}^J$ are the basics of SCMA. For $K = 4$, $J = 6$ and $N_j = 2$, ($j = 1, \dots, J$), an example of resource assignment matrix is given by

$$\mathbf{F}_{4,6} = \begin{bmatrix} 1 & 1 & 1 & 0 & 0 & 0 \\ 1 & 0 & 0 & 1 & 1 & 0 \\ 0 & 1 & 0 & 1 & 0 & 1 \\ 0 & 0 & 1 & 0 & 1 & 1 \end{bmatrix}. \quad (1)$$

The second column of \mathbf{F} , for example, spreads $c_2 = [c_{1,2} \ c_{2,2}]^T$ into $x_2 = [c_{1,2} \ 0 \ c_{2,2} \ 0]^T$.

Note that for $\sum_{j=1}^J N_j > K$, the system is overloaded, since in this case, an orthogonal sharing of the K resources among the users is impossible. The number of zeros in the j th column of \mathbf{F} is equal to $K - N_j$. Therefore, the sparsity of \mathbf{F} is determined by N_j , $1 \leq j \leq J$. Intuitively, a denser \mathbf{F} , i.e., less zeros, will attain a higher bit rate since more bits are transmitted per channel use, but its BER performance will be poorer due to a higher IUI.

¹In line with the current cellular network standards, we assume that neighboring cells do not share the same resources and, therefore, only intra-cell interference needs to be considered and the system becomes effectively a single-cell one. However, our approach can be extended to the inter-cell-interference scenario where neighboring cells reuse the same resources.

The transmit signals based on the K orthogonal resources for the J users propagate through the J channels and are combined at the BS to yield the received signal vector $\mathbf{y} \in \mathbb{C}^K$

$$\mathbf{y} = \sum_{j=1}^J \text{diag}(\mathbf{h}_j) \mathbf{x}_j + \mathbf{n}, \quad (2)$$

where $\mathbf{h}_j \in \mathbb{C}^K$ whose elements are the channel gains of the K orthogonal resources for the j th user, and \mathbf{n} is the additive white Gaussian noise (AWGN) vector with the zero mean vector and the covariance matrix of $\sigma_n^2 \mathbf{I}_K$. Let $p_{k,j} = E\{x_{k,j}^* x_{k,j}\}$ be the average power of the k th element of $\mathbf{x}_j = [x_{1,j} \ \dots \ x_{K,j}]^T$. Clearly, $p_{k,j} = 0$ if $f_{k,j} = 0$, where $f_{k,j}$ is the k th-row and j th-column element of the resource assignment matrix \mathbf{F} .

The main advantage of SCMA over CDMA stems from its multi-dimensional constellation design, which results in a shaping gain, particularly for the heavy overload case of $J > K$. The transmit signal vector $\tilde{\mathbf{x}}_j \in \mathbb{C}^K$ for CDMA can be written as $\tilde{\mathbf{x}}_j = \mathbf{s}_j \cdot d_j$, where $\mathbf{s}_j \in \mathbb{C}^K$ is the spreading sequence for user j and d_j is the one-dimensional constellation symbol with unitary average power. The design of the multi-dimensional constellation \mathcal{C}_j for SCMA is much more flexible than the design of one-dimensional constellation for CDMA. In the next section, we will show that given the same K orthogonal resources and the same power allocation matrix, SCMA can achieve higher throughput than CDMA.

III. CAPACITY REGION FOR SCMA SYSTEM

Given the channel state $\mathbf{H} = \{\mathbf{h}_j\}_{j=1}^J$ and the power allocation function or matrix \mathbf{P} for all the users whose k th-row and j th-column elements are denoted by $p_{k,j}$ for $1 \leq k \leq K$ and $1 \leq j \leq J$, the capacity region for MACs is shown to be [29]

$$\mathcal{C}_{\text{MAC}}(\mathbf{P}, \mathbf{H}) = \left\{ \mathbf{R} : \sum_{j \in \mathcal{S}} R_j \leq I(\mathbf{x}_j, j \in \mathcal{S}; \mathbf{y} | \mathbf{x}_k, k \notin \mathcal{S}), \right. \\ \left. \mathcal{S} \subset \{1, \dots, J\} \right\}, \quad (3)$$

where the data rate vector $\mathbf{R} = [R_1 \ R_2 \ \dots \ R_J]^T$ in which R_j represents the rate for user j that is achievable with a practical codebook design \mathcal{C}_j of a specific $N_{B,j}$ value, while the average mutual information (MI) $I(\mathbf{x}_j, j \in \mathcal{S}; \mathbf{y} | \mathbf{x}_k, k \notin \mathcal{S})$ can be calculated according to (4) given at the bottom of the next page. Accordingly, the capacity region for the SCMA system is given by (5) at the bottom of the next page. The capacity region $\mathcal{C}_{\text{SCMA}}(\mathbf{P}, \mathbf{H})$ represents the upper bound or maximum achievable rates of all the users. Note that the capacity is independent of any practical codebook design \mathcal{C}_j . Observe however that the upper bound in (4) is reached, that is, the last inequality of (4) becomes the equality, when the autocorrelation matrices of \mathbf{x}_j are diagonal

$$E\{\mathbf{x}_j \mathbf{x}_j^H\} = \text{diag}(p_{1,j}, \dots, p_{K,j}), \quad 1 \leq j \leq J. \quad (6)$$

Clearly, $E\{\mathbf{x}_j \mathbf{x}_j^H\}$ are diagonal if the code vectors c_j have diagonal covariance matrices. This offers an 'optimal' practical SCMA codebook design with respect to the maximum achievable data rates or capacity. Specifically, one should

design the SCMA constellations \mathcal{C}_j so that the autocorrelation matrices of \mathbf{c}_j are diagonal, because this design is capable of improving the capacity over any other practical codebook design. Consider the example of $K = 4$, $J = 6$ and $N_j = 2$, $1 \leq j \leq J$, given in the previous section. Assume that $N_{B,j} = 2$ bits, $1 \leq j \leq 6$. By designing the two-dimensional practical constellation \mathcal{C}_j to be

$$\left\{ \begin{bmatrix} 1+j \\ -1-j \end{bmatrix}, \begin{bmatrix} 1-j \\ 1-j \end{bmatrix}, \begin{bmatrix} -1+j \\ -1+j \end{bmatrix}, \begin{bmatrix} -1-j \\ 1+j \end{bmatrix} \right\}, \quad (7)$$

the autocorrelation matrix $E\{\mathbf{c}_j \mathbf{c}_j^H\} = 2\mathbf{I}_2$.

Given the same K orthogonal resources with $K < J$, the same channel state and the same power allocation function, according to [8], the capacity region for CDMA is expressed as (8) at the bottom of this page, in which $\widetilde{\mathbf{H}}_S \widetilde{\mathbf{H}}_S^H$ is given in (9), as shown at the bottom of this page. According to the Hadamard inequality, $\det(\mathbf{A}) \leq \prod_{i=1}^K a_{i,i}$ if $\mathbf{A} \in \mathbb{C}^{K \times K}$ is a positive definite matrix [32]. The ‘upper bound’ of $\sum_{j \in \mathcal{S}} \text{diag}(\mathbf{h}_j) E\{\mathbf{s}_j \mathbf{s}_j^H\} (\text{diag}(\mathbf{h}_j))^H$ cannot be reached, since $E\{\mathbf{s}_j \mathbf{s}_j^H\}$ is not diagonal. By contrast, the ‘upper bound’ of $\sum_{j \in \mathcal{S}} \text{diag}(\mathbf{h}_j) E\{\mathbf{x}_j \mathbf{x}_j^H\} (\text{diag}(\mathbf{h}_j))^H$ for SCMA can be reached. Thus the upper bound of the SCMA sum rate is larger than that of the CDMA sum rate, that is, the capacity region of the CDMA system is a subset of that for the SCMA system. This is why SCMA is able to achieve larger data rate than CDMA.

Any data rate vector \mathbf{R} in the capacity region (5) is the combination of all the users’ rates that are achievable under the channel state \mathbf{H} and the power allocation function \mathbf{P} with a given codebook. The achievable data rates for different users have coupling influence on each other. As illustrated in Fig. 2, points A and B are both at the boundary of the capacity region. At point A, user 2 achieves a higher data rate than at point B, since the data rate of user 1 at point A is lower than at point B. Therefore, a data rate allocation function is needed to decide the suitable data rate vector within the capacity region. The capacity region given in (5) has many attractive properties. For example, it is a convex polynomial with respect to the rate vector \mathbf{R} given the power allocation function \mathbf{P} . For a fixed-rate vector \mathbf{R} , since the sum of logarithm functions

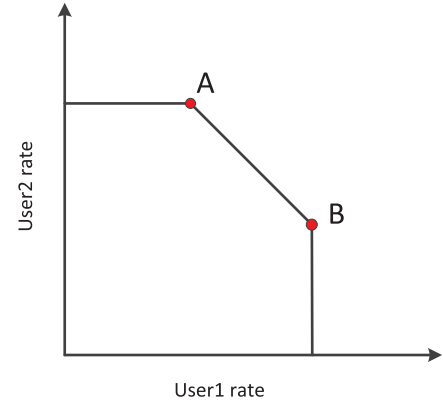


Fig. 2. An example of capacity region for the SCMA system with two users.

is concave, (5) represents a convex set with respect to \mathbf{P} . Furthermore, given \mathbf{F} , the capacity region is convex with respect to \mathbf{R} and \mathbf{P} jointly.

The convexity of (5) facilitates effectively data rate allocation. The optimization problem with respect to the rate vector and power allocation function is formulated as

$$\begin{aligned} & \max_{\mathbf{P}, \mathbf{R}} g(\mathbf{R}, \mathbf{P}), \\ & \text{s.t. } u(\mathbf{P}) \leq \bar{\mathbf{P}}, \\ & \mathbf{R} \in C_{\text{SCMA}}(\mathbf{P}, \mathbf{H}), \end{aligned} \quad (10)$$

where $g(\mathbf{R}, \mathbf{P})$ is the objective function, $u(\mathbf{P})$ is a linear power constraint function and $\bar{\mathbf{P}}$ is the corresponding predefined power constraint. For example, if the sum power constraint is considered, $u(\mathbf{P})$ is the sum of all the elements of \mathbf{P} , with $\bar{\mathbf{P}} = \bar{P}$ being a positive scalar. On the other hand, when the individual user power constraints are imposed, $u(\mathbf{P})$ is the J -dimensional positive real vector, and all the elements of $\bar{\mathbf{P}} = [\bar{P}_1 \cdots \bar{P}_J]^T$ are real and positive.

Clearly, the sparsity of the resource assignment matrix \mathbf{F} influences the capacity region (5). For a sparser \mathbf{F} , i.e., less number of $f_{k,j} = 1$, the upper bound $\sum_{k=1}^K \log \left(1 + \frac{1}{\sigma_n^2} \sum_{j \in \mathcal{S}} |h_{k,j}|^2 p_{k,j} f_{k,j} \right)$ in (5) is smaller and, therefore, the achievable rate is smaller. But a sparser \mathbf{F} means less IUI and, therefore, the complexity of the multi-user

$$I(\mathbf{x}_j, j \in \mathcal{S}; \mathbf{y} | \mathbf{x}_k, k \notin \mathcal{S}) = \log \left(\det \left(\mathbf{I}_K + \frac{1}{\sigma_n^2} \sum_{j \in \mathcal{S}} \text{diag}(\mathbf{h}_j) E\{\mathbf{x}_j \mathbf{x}_j^H\} (\text{diag}(\mathbf{h}_j))^H \right) \right) \leq \sum_{k=1}^K \log \left(1 + \frac{1}{\sigma_n^2} \sum_{j \in \mathcal{S}} |h_{k,j}|^2 p_{k,j} f_{k,j} \right). \quad (4)$$

$$C_{\text{SCMA}}(\mathbf{P}, \mathbf{H}) = \left\{ \mathbf{R} : \sum_{j \in \mathcal{S}} R_j \leq \sum_{k=1}^K \log \left(1 + \frac{1}{\sigma_n^2} \sum_{j \in \mathcal{S}} |h_{k,j}|^2 p_{k,j} f_{k,j} \right), \mathcal{S} \subset \{1, \dots, J\} \right\} \quad (5)$$

$$C_{\text{CDMA}}(\mathbf{P}, \mathbf{H}) = \left\{ \mathbf{R} : \sum_{j \in \mathcal{S}} R_j \leq \log \left(\det \left(\mathbf{I}_K + \frac{1}{\sigma_n^2} \widetilde{\mathbf{H}}_S \widetilde{\mathbf{H}}_S^H \right) \right), \mathcal{S} \subset \{1, \dots, J\} \right\}, \quad (8)$$

$$\widetilde{\mathbf{H}}_S \widetilde{\mathbf{H}}_S^H = \sum_{j \in \mathcal{S}} \text{diag}(\mathbf{h}_j) E\{\tilde{\mathbf{x}}_j \tilde{\mathbf{x}}_j^H\} (\text{diag}(\mathbf{h}_j))^H = \sum_{j \in \mathcal{S}} \text{diag}(\mathbf{h}_j) E\{\mathbf{s}_j \mathbf{s}_j^H\} (\text{diag}(\mathbf{h}_j))^H. \quad (9)$$

$$C_{\text{out}}(\bar{\mathbf{P}}, Pr_{\text{th}}) \triangleq \bigcup_{\forall \mathcal{P}^{\text{rand}}: E\{u(\mathbf{P}^{\text{rand}}(\mathbf{H}))\} \leq \bar{\mathbf{P}}} \{\mathbf{R} : \Pr[\mathbf{R} \in C_{\text{SCMA}}(\mathbf{P}^{\text{rand}}(\mathbf{H}), \mathbf{H})] \geq 1 - Pr_{\text{th}}\}. \quad (11)$$

detection will be smaller. Since the power allocation $p_{k,j}$ for user j at the k th orthogonal resource is only needed if $f_{k,j} = 1$, the number of effective power allocation elements in the $K \times J$ -dimensional \mathbf{P} is actually equal to the number of ones in \mathbf{F} . Therefore, a sparser \mathbf{F} also reduces the complexity of the optimization problem (10).

IV. COMMON OUTAGE PROBABILITY

In a slow-fading environment, the outage probability is an important metric to evaluate a power allocation policy. As in [30], the set of all randomized power allocation policies are investigated in this paper. For a randomized power allocation policy $\mathcal{P}^{\text{rand}}$, the transmit power allocation matrix $\mathbf{P}^{\text{rand}}(\mathbf{H})$ for the channel state \mathbf{H} is a continuous random variable with the joint probability density function (PDF) or a discrete random variable with the joint probability mass function (PMF) $f_{\mathbf{P}^{\text{rand}}}(\mathbf{H})$. Note that the positions or indices of zeros in $\mathbf{P}^{\text{rand}}(\mathbf{H})$ are specified by the resource assignment policy or matrix \mathbf{F} . Thus, similar to [30], the common outage probability of \mathbf{R} given a power allocation policy $\mathcal{P}^{\text{rand}}$ is defined as the probability that \mathbf{R} is outside the capacity region $C_{\text{SCMA}}(\mathbf{P}^{\text{rand}}(\mathbf{H}), \mathbf{H})$. Accordingly, the common outage capacity region is defined as the set of rate vectors whose common outage probabilities can be maintained under a threshold Pr_{th} with the power allocation policy $\mathcal{P}^{\text{rand}}$ satisfying $E\{u(\mathbf{P}^{\text{rand}}(\mathbf{H}))\} \leq \bar{\mathbf{P}}$ [30], [33]. That is, the common outage capacity region is defined by (11) given at the top of this page.

Given the power constraint $\bar{\mathbf{P}}$, the common outage probability region for a fixed data rate \mathbf{R} , denoted by $\mathcal{O}_C(\bar{\mathbf{P}}, \mathbf{R})$, is defined as the set of outage probabilities whose elements Pr_{out} satisfy $\mathbf{R} \in C_{\text{out}}(\bar{\mathbf{P}}, Pr_{\text{out}})$, while the common usage probability region $\bar{\mathcal{O}}_C(\bar{\mathbf{P}}, \mathbf{R})$ defines the set of usage probabilities Pr_{usa} that satisfy $\mathbf{R} \in C_{\text{out}}(\bar{\mathbf{P}}, 1 - Pr_{\text{usa}})$ [30].

However, the above definitions are hard to compute, since the set of all the randomized power allocation policies are too large to tackle directly. Similar to [30], we will only consider the set of the power allocation policies having the form

$$\mathbf{P}^{\text{rand}}(\mathbf{H}) = \begin{cases} \mathbf{0}, & \text{with probability } 1 - w(\mathbf{H}), \\ \mathbf{P}(\mathbf{H}), & \text{with probability } w(\mathbf{H}), \end{cases} \quad (12)$$

where $w(\mathbf{H})$ is the probability that the power allocation function takes the value of $\mathbf{P}(\mathbf{H})$. We have the following proposition. The proof of this proposition is similar to

the proof of the outage probability region for Gaussian MACs [30].

Proposition 1: Given the resource assignment policy \mathbf{F} , the common usage probability region for SCMA systems is given by (13) at the bottom of this page.

According to its definition and Proposition 1, the common usage probability region is a convex set. In fact, it is easy to show that $\bar{\mathcal{O}}_C(\bar{\mathbf{P}}, \mathbf{R}) = [0, Pr_{\text{usa,max}}]$. Equivalently, the common outage probability region $\mathcal{O}_C(\bar{\mathbf{P}}, \mathbf{R}) = [Pr_{\text{out,min}}, 1]$, where $Pr_{\text{out,min}} = 1 - Pr_{\text{usa,max}}$. Therefore, determining the common outage probability region is equivalent to finding the minimum common outage probability $Pr_{\text{out,min}}$, which is in turn equivalent to finding the maximum common usage probability $Pr_{\text{usa,max}}$. The maximum common usage probability is calculated as

$$\begin{aligned} \max \quad & Pr_{\text{usa}}, \\ \text{s.t.} \quad & Pr_{\text{usa}} \in \bar{\mathcal{O}}_C(\bar{\mathbf{P}}, \mathbf{R}), \end{aligned} \quad (14)$$

which can be rewritten as

$$\begin{aligned} \max_{(Pr_{\text{usa}}, \mathbf{P}_c) \in \mathcal{Q}_C(\mathbf{R})} \quad & Pr_{\text{usa}}, \\ \text{s.t.} \quad & \mathbf{P}_c \leq \bar{\mathbf{P}}, \end{aligned} \quad (15)$$

where

$$\mathcal{Q}_C(\mathbf{R}) \triangleq \{(Pr_{\text{usa}}, \mathbf{P}_c) : Pr_{\text{usa}} \in \bar{\mathcal{O}}_C(\mathbf{P}_c, \mathbf{R})\}. \quad (16)$$

Lemma 1: The feasible region of the optimization problem (15) contains interior points.

Proof: See Appendix A. ■

Similar to [30], $\mathcal{Q}_C(\mathbf{R})$ can be proven to be convex. Therefore, (15) is a convex optimization problem with a linear objective function and a convex feasible region. Since the feasible region of (15) has interior points, the optimization (15) is equivalent to its Lagrangian dual problem. Replacing Pr_{usa} with $E\{w(\mathbf{H})\}$ and \mathbf{P}_c with $E\{w(\mathbf{H})u(\mathbf{P}(\mathbf{H}))\}$ according to Proposition 1, the Lagrangian dual function is given in (17) at the bottom of this page. where λ_C is the Lagrangian multiplier vector. Given λ_C , the optimal $\mathbf{P}_{\lambda_C}^*(\mathbf{H})$ and $w_{\lambda_C}^*(\mathbf{H})$ for (17) can be obtained through solving the following two

$$\bar{\mathcal{O}}_C(\bar{\mathbf{P}}, \mathbf{R}) = \bigcup_{\{w(\mathbf{H}), \mathbf{P}(\mathbf{H}) : E\{w(\mathbf{H})u(\mathbf{P}(\mathbf{H}))\} \leq \bar{\mathbf{P}}, \mathbf{R} \in C_{\text{SCMA}}(\mathbf{P}(\mathbf{H}), \mathbf{H}), \forall \mathbf{H} : w(\mathbf{H}) > 0\}} E\{w(\mathbf{H})\} \quad (13)$$

$$\begin{aligned} L(\lambda_C) = \quad & \max_{0 \leq w(\mathbf{H}) \leq 1, \mathbf{P}(\mathbf{H}) \geq \mathbf{0}} E\{w(\mathbf{H})\} - \lambda_C^T (E\{w(\mathbf{H})u(\mathbf{P}(\mathbf{H}))\} - \bar{\mathbf{P}}) \\ \text{s.t.} \quad & \mathbf{R} \in C_{\text{SCMA}}(\mathbf{P}(\mathbf{H}), \mathbf{H}), \quad \forall \mathbf{H} : w(\mathbf{H}) > 0, \end{aligned} \quad (17)$$

$$L(\boldsymbol{\lambda}_C, \mu_C) = \max_{v, 0 \leq w(\mathbf{H}) \leq 1, \mathbf{P}(\mathbf{H}) \geq 0} q_C(v) - \mu_C(v - E\{w(\mathbf{H})\}) - \boldsymbol{\lambda}_C^T (E\{w(\mathbf{H})u(\mathbf{P}(\mathbf{H}))\} - \bar{\mathbf{P}}),$$

$$\text{s.t. } 0 \leq v \leq 1,$$

$$\mathbf{R} \in C_{\text{SCMA}}(\mathbf{P}(\mathbf{H}), \mathbf{H}), \forall \mathbf{H} : w(\mathbf{H}) > 0. \quad (23)$$

optimal problems in sequence

$$\min_{\mathbf{P}(\mathbf{H}) \geq 0} \boldsymbol{\lambda}_C^T u(\mathbf{P}(\mathbf{H})),$$

$$\text{s.t. } \mathbf{R} \in C_{\text{SCMA}}(\mathbf{P}(\mathbf{H}), \mathbf{H}), \quad (18)$$

$$\max_{0 \leq w(\mathbf{H}) \leq 1} w(\mathbf{H})(1 - \boldsymbol{\lambda}_C^T u(\mathbf{P}_{\boldsymbol{\lambda}_C}^*(\mathbf{H}))). \quad (19)$$

Note that the solution to the optimization (19) is given explicitly by the closed form

$$w^*(\mathbf{H}) = \begin{cases} 1, & \boldsymbol{\lambda}_C^T u(\mathbf{P}_{\boldsymbol{\lambda}_C}^*(\mathbf{H})) \leq 1, \\ 0, & \boldsymbol{\lambda}_C^T u(\mathbf{P}_{\boldsymbol{\lambda}_C}^*(\mathbf{H})) > 1, \end{cases} \quad (20)$$

which is one of the two boundary points of the feasible region. Different from the Gaussian MAC system of [30], there is no analytical solution to (18) but the optimization (18) can be solved numerically with the efficient convex programming algorithms [34].

Then, similar to [30], the dual problem $\min_{\boldsymbol{\lambda}_C} L(\boldsymbol{\lambda}_C)$ can be solved by the descent algorithm

$$\boldsymbol{\lambda}_C[n+1] = (\boldsymbol{\lambda}_C[n] + \alpha (E\{w_n^C(\mathbf{H})u(\mathbf{P}_n^C(\mathbf{H}))\} - \bar{\mathbf{P}}))_\varepsilon^+, \quad (21)$$

where $\mathbf{P}_n^C(\mathbf{H})$ and $w_n^C(\mathbf{H})$ are the solutions to (18) and (19), respectively, given $\boldsymbol{\lambda}_C[n]$ and channel state \mathbf{H} , while α is the step size, and ε is a small positive scalar to prevent the elements of $\boldsymbol{\lambda}_C[n+1]$ too close to zero for the robustness purpose. After a number of iterations, $\boldsymbol{\lambda}_C[n]$ converges to the optimal value $\boldsymbol{\lambda}_C^*$, and the maximum common usage probability is given as $E\{w_{\boldsymbol{\lambda}_C^*}^*(\mathbf{H})\}$. Note that the expectation operation is required to calculate the expectation $E\{w_n^C(\mathbf{H})u(\mathbf{P}_n^C(\mathbf{H}))\}$ in each iteration and also in the calculation of the optimal usage probability, which is extremely time consuming and costly.

V. PROPOSED ADAPTIVE ALGORITHM FOR OUTAGE PROBABILITY CALCULATION

To avoid the costly expectation operation, we first modify the optimization problem (15). Specifically, by considering a monotonically increasing concave function $q_C(v)$ for $0 \leq v \leq 1$, the optimization problem (15) can be rewritten equivalently as

$$\max_{0 \leq v \leq 1, (\mathbf{P}_{\text{usa}}, \mathbf{P}_c) \in \mathcal{Q}_C(\mathbf{R})} q_C(v),$$

$$\text{s.t. } v = Pr_{\text{usa}},$$

$$\mathbf{P}_c \leq \bar{\mathbf{P}}. \quad (22)$$

Since the additional constraint is a linear equality constraint and the objective function is concave, (22) is a convex optimization problem. Moreover, the feasible region of (22) has

interior points, which can be proved similarly as in the proof of Lemma 1. Therefore, (22) is equivalent to its Lagrangian dual problem. Again, replacing Pr_{usa} and \mathbf{P}_c with $E\{w(\mathbf{H})\}$ and $E\{w(\mathbf{H})u(\mathbf{P}(\mathbf{H}))\}$, the Lagrangian dual function is expressed as (23) given at the top of this page. Given $\boldsymbol{\lambda}_C$ and μ_C , the optimal $v_{\boldsymbol{\lambda}_C, \mu_C}^*$, $\mathbf{P}_{\boldsymbol{\lambda}_C, \mu_C}^*(\mathbf{H})$ and $w_{\boldsymbol{\lambda}_C, \mu_C}^*(\mathbf{H})$ are attainable by solving the following three optimization problems in sequence

$$\max_{0 \leq v \leq 1} q_C(v) - \mu_C v, \quad (24)$$

$$\min_{\mathbf{P}(\mathbf{H}) \geq 0} \boldsymbol{\lambda}_C^T u(\mathbf{P}(\mathbf{H})),$$

$$\text{s.t. } \mathbf{R} \in C_{\text{SCMA}}(\mathbf{P}(\mathbf{H}), \mathbf{H}), \quad (25)$$

$$\max_{0 \leq w(\mathbf{H}) \leq 1} w(\mathbf{H})(\mu_C - \boldsymbol{\lambda}_C^T u(\mathbf{P}_{\boldsymbol{\lambda}_C, \mu_C}^*(\mathbf{H}))). \quad (26)$$

Then, the optimal Lagrange multipliers $\boldsymbol{\lambda}_C^*$ and μ_C^* can be obtained iteratively with the descent algorithm

$$\begin{cases} \boldsymbol{\lambda}_C[n+1] = (\boldsymbol{\lambda}_C[n] + \alpha (E\{w_n^C(\mathbf{H})u(\mathbf{P}_n^C(\mathbf{H}))\} - \bar{\mathbf{P}}))_\varepsilon^+, \\ \mu_C[n+1] = (\mu_C[n] + \alpha (v_n^C - E\{w_n^C(\mathbf{H})\}))_\varepsilon^+, \end{cases} \quad (27)$$

where v_n^C , $\mathbf{P}_n^C(\mathbf{H})$, and $w_n^C(\mathbf{H})$ are the solutions to (24), (25) and (26), respectively, given $\boldsymbol{\lambda}_C[n]$, $\mu_C[n]$ and \mathbf{H} . Once the optimal Lagrange multipliers are obtained, the optimal result of the dual problem is equivalent to the optimal result of the original problem.

Compared with (21), a new Lagrange multiplier μ_C is added in (27). It is worth noting that given μ_C^* , as long as the function $q_C(\cdot)$ is strictly concave so that the solution to (26) is unique, the solution $v_{\boldsymbol{\lambda}_C^*, \mu_C^*}^*$ to (24) satisfies $v_{\boldsymbol{\lambda}_C^*, \mu_C^*}^* = Pr_{\text{usa}}^* = E\{w_{\boldsymbol{\lambda}_C^*, \mu_C^*}^*(\mathbf{H})\}$ according to the property of the Lagrangian dual method [35]. Thus the maximum usage probability can be obtained as the optimal $v_{\boldsymbol{\lambda}_C^*, \mu_C^*}^*$, without having to calculate the expectation of $w_{\boldsymbol{\lambda}_C^*, \mu_C^*}^*(\mathbf{H})$. By further omitting the expectation operation in (27), we convert it to

$$\begin{cases} \hat{\boldsymbol{\lambda}}_C[n+1] = (\hat{\boldsymbol{\lambda}}_C[n] + \alpha (w_n^C(\mathbf{H}[n])u(\mathbf{P}_n^C(\mathbf{H}[n])) - \bar{\mathbf{P}}))_\varepsilon^+, \\ \hat{\mu}_C[n+1] = (\hat{\mu}_C[n] + \alpha (v_n^C - w_n^C(\mathbf{H}[n])))_\varepsilon^+, \end{cases} \quad (28)$$

where $\mathbf{H}[n]$ is the instantaneous channel state in the n -th iteration, which is drawn from a distribution with the given cumulative distribution function (CDF).

Although uncertainty is introduced in (28) due to removing the expectation operation, the difference between the solutions of the two iterative descent algorithms (27) and (28) is bounded. Denote the Lagrange multipliers calculated

according to (27) and (28) as

$$\mathbf{\Lambda}[n] \triangleq [\mu_C[n] \boldsymbol{\lambda}_C^T[n]]^T, \quad (29)$$

$$\widehat{\mathbf{\Lambda}}[n] \triangleq [\widehat{\mu}_C[n] \widehat{\boldsymbol{\lambda}}_C^T[n]]^T, \quad (30)$$

respectively. We have the following lemma.

Lemma 2: For the ergodic fading channel with a continuous CDF, assume that the descent algorithm (27) and its adaptive version (28) have the same initialization. Then

$$\max_{1 \leq n \leq T/\alpha} \|\widehat{\mathbf{\Lambda}}[n] - \mathbf{\Lambda}[n]\| \leq c_T(\alpha) \quad (31)$$

holds for any time interval T , where $c_T(\alpha) \rightarrow 0$ as $\alpha \rightarrow 0$.

Proof: See Appendix B. ■

Lemma 2 shows that for sufficiently small step size α , $\widehat{\mathbf{\Lambda}}[n]$ is sufficiently close to $\mathbf{\Lambda}[n]$. It is well known that for sufficiently small α , $\mathbf{\Lambda}[n]$ is guaranteed to converge to the optimal value $\mathbf{\Lambda}^*$. Consequently, Lemma 2 proves that $\widehat{\mathbf{\Lambda}}[n] \rightarrow \mathbf{\Lambda}^*$ as $n \rightarrow \infty$, for sufficiently small α .

Remark 1: Compared to the descent algorithm (27), the adaptive version (28) is a much more practical method of obtaining the optimal Lagrange multipliers, as the calculation in each iteration is based on the instantaneous channel state, not the expectation over the channel state which is costly and time consuming to approximate. Note that a power allocation policy $\{w_{\lambda_C^*}^*(\mathbf{H}), \mathbf{P}_{\lambda_C^*}^*(\mathbf{H})\}$ in the form of (12) is naturally obtained via the optimizations (25) and (26), which is able to achieve the optimal outage (usage) probability. Specifically, after obtaining the optimal Lagrange multipliers $\boldsymbol{\lambda}_C^*$, we can calculate the power allocation function $\mathbf{P}_{\lambda_C^*}^*(\mathbf{H})$ and its probability $w_{\lambda_C^*}^*(\mathbf{H})$ according to (25) and (26) for any channel state \mathbf{H} . If $w_{\lambda_C^*}^*(\mathbf{H}) > 0$, the power allocation function $\mathbf{P}_{\lambda_C^*}^*(\mathbf{H})$ is applied to the users with the probability $w_{\lambda_C^*}^*(\mathbf{H})$. Otherwise, we do not transmit signals in this time slot since the channel state is poor. After the dual variables converge, this power allocation policy achieves the optimal outage (usage) probability. Moreover, since the Lagrange multipliers are updated based on the instantaneous channel state, the proposed algorithm is capable of tracking the variation of the underlying channel state distribution to adapt the optimal outage probability and power allocation policy.

VI. INDIVIDUAL OUTAGE PROBABILITY

Since the data for different users are transmitted independently, the individual outage probabilities are also important. Actually, the investigation of the individual outage probabilities is an extension of that for the common outage probability [30]. Again, the set of all randomized power allocation policies are considered. When a power allocation policy $\mathcal{P}^{\text{rand}}$ with the transmit power allocation matrix $\mathbf{P}^{\text{rand}}(\mathbf{H})$ and a data rate allocation function $\mathbf{R}(\mathbf{P}, \mathbf{H}) = [R_1(\mathbf{P}, \mathbf{H}) R_2(\mathbf{P}, \mathbf{H}) \cdots R_J(\mathbf{P}, \mathbf{H})]^T \in C_{\text{SCMA}}(\mathbf{P}, \mathbf{H})$ are adopted, the outage probability of the j -th user's data rate is defined by

$$Pr_{\text{out},j} = \Pr [R_j > R_j(\mathbf{P}^{\text{rand}}(\mathbf{H}), \mathbf{H})], \quad 1 \leq j \leq J, \quad (32)$$

which form the individual outage probability vector $\mathbf{Pr}_{\text{out}} = [Pr_{\text{out},1} Pr_{\text{out},2} \cdots Pr_{\text{out},J}]^T$.

The individual outage capacity region $C_{\text{out}}^I(\bar{\mathbf{P}}, \mathbf{Pr}_{\text{th}})$ is defined as the set of data rate vectors whose individual outage probability vectors are controlled under the threshold \mathbf{Pr}_{th} with power allocation policy $\mathbf{P}^{\text{rand}}(\mathbf{H})$ and rate allocation function $\mathbf{R}(\mathbf{P}^{\text{rand}}(\mathbf{H}), \mathbf{H})$, where the power allocation policy satisfies the power constraint $E\{u(\mathbf{P}^{\text{rand}}(\mathbf{H}))\} \leq \bar{\mathbf{P}}$. Similar to the definitions of the common outage probability region $\mathcal{O}_C(\bar{\mathbf{P}}, \mathbf{R})$ and the common usage probability region $\bar{\mathcal{O}}_C(\bar{\mathbf{P}}, \mathbf{R})$, we can also define the individual outage probability region $\mathcal{O}_I(\bar{\mathbf{P}}, \mathbf{R})$ and the individual usage probability region $\bar{\mathcal{O}}_I(\bar{\mathbf{P}}, \mathbf{R})$. Obviously, $\mathcal{O}_I(\bar{\mathbf{P}}, \mathbf{R})$ and $\bar{\mathcal{O}}_I(\bar{\mathbf{P}}, \mathbf{R})$ are equivalent, since $\mathbf{Pr} \in \mathcal{O}_I(\bar{\mathbf{P}}, \mathbf{R}) \Leftrightarrow \mathbf{1}_J - \mathbf{Pr} \in \bar{\mathcal{O}}_I(\bar{\mathbf{P}}, \mathbf{R})$.

Owing to the convexity of the SCMA capacity region C_{SCMA} , $\mathcal{O}_I(\bar{\mathbf{P}}, \mathbf{R})$ and $\bar{\mathcal{O}}_I(\bar{\mathbf{P}}, \mathbf{R})$ can be simply represented by the random power allocation policies of cardinality 2^J per fading channel, similar to the individual outage capacity region of Gaussian MACs [30]. Before defining these power allocation policies, we note that there are a total of 2^J combinations or subsets of the users' index set $\{1, 2, \dots, J\}$, namely, the null set \mathcal{S}_0 , which does not contain any user, and

$$\mathcal{S}_m \subseteq \{1, 2, \dots, J\}, \quad 1 \leq m \leq 2^J - 1. \quad (33)$$

Correspondingly, we introduce the binary indicator vector $\boldsymbol{\psi}(m) = [\psi_1(m) \psi_2(m) \cdots \psi_J(m)]^T$, for each subset \mathcal{S}_m , $0 \leq m \leq 2^J - 1$, where for $1 \leq j \leq J$,

$$\psi_j(m) = \begin{cases} 1, & \text{user } j \text{ belongs to } \mathcal{S}_m, \\ 0, & \text{otherwise.} \end{cases} \quad (34)$$

Clearly, we have $\boldsymbol{\psi}(0) = \mathbf{0}$. Then, we consider the random power policies with the form of

$$\mathcal{P}^I : \mathbf{P}^{\text{rand}}(\mathbf{H}) = \begin{cases} \mathbf{0}, & \text{with probability } w(\mathbf{H}, 0), \\ \mathbf{P}(\mathbf{H}, m), & \text{with probability } w(\mathbf{H}, m), \\ & 1 \leq m \leq 2^J - 1, \end{cases} \quad (35)$$

where $0 \leq w(\mathbf{H}, m) \leq 1$ is the probability that the power allocation function takes the value $\mathbf{P}(\mathbf{H}, m)$ and $\sum_{m=0}^{2^J-1} w(\mathbf{H}, m) = 1$, while the power allocation scheme $\mathbf{P}(\mathbf{H}, m)$ corresponds to the powers allocated to the users in the subset \mathcal{S}_m . Specifically, $p_{k,j}(\mathbf{H}, m)$, $1 \leq k \leq K$, are the powers allocated to the transmit signal of the j -th user in the subset \mathcal{S}_m . Clearly, if $\psi_j(m) = 0$, $p_{k,j}(\mathbf{H}, m) = 0$ for $1 \leq k \leq K$.

We have the following proposition for $\bar{\mathcal{O}}_I(\mathbf{P}, \mathbf{R})$. The proof of this proposition is similar to the proof for Gaussian MACs given in [30].

Proposition 2: Given the resource assignment policy \mathbf{F} , the individual usage probability region $\bar{\mathcal{O}}_I(\mathbf{P}, \mathbf{R})$ for SCMA systems can be expressed as

$$\bar{\mathcal{O}}_I(\bar{\mathbf{P}}, \mathbf{R}) = \bigcup_{w(\mathbf{H}, m), \mathbf{P}(\mathbf{H}, m) \geq \mathbf{0}, \forall m} E\{\mathbf{w}(\mathbf{H})\}, \quad (36)$$

$$L(\lambda_I, \mu_I) = \max_{\mathbf{0} \leq \mathbf{v} \leq \mathbf{1}_J, \mathbf{0} \leq w(\mathbf{H}, m) \leq 1, \mathbf{P}(\mathbf{H}, m) \geq \mathbf{0}, \forall m} q_I(\mathbf{v}) - \mu_I^T (\mathbf{v} - E\{\mathbf{w}(\mathbf{H})\}) - \lambda_I^T \left(E \left\{ \sum_{m=1}^{2^J-1} w(\mathbf{H}, m) u(\mathbf{P}(\mathbf{H}, m)) \right\} - \bar{\mathbf{P}} \right),$$

$$\text{s.t. } \sum_{m=0}^{2^J-1} w(\mathbf{H}, m) = 1,$$

$$\psi(m) \odot \mathbf{R} \in C_{\text{SCMA}}(\mathbf{P}(\mathbf{H}, m), \mathbf{H}), \quad \forall \mathbf{H}, m : w(\mathbf{H}, m) > 0. \quad (43)$$

where

$$\mathbf{w}(\mathbf{H}) \triangleq \sum_{m=0}^{2^J-1} w(\mathbf{H}, m) \psi(m), \quad (37)$$

$$E \left\{ \sum_{m=1}^{2^J-1} w(\mathbf{H}, m) u(\mathbf{P}(\mathbf{H}, m)) \right\} \leq \bar{\mathbf{P}}, \quad (38)$$

$$\psi(k) \odot \mathbf{R} \in C_{\text{SCMA}}(\mathbf{P}(\mathbf{H}, m), \mathbf{H}),$$

$$\forall \mathbf{H}, m : w(\mathbf{H}, m) > 0. \quad (39)$$

$\bar{\mathcal{O}}_I(\bar{\mathbf{P}}, \mathbf{R})$ is a convex set. Moreover, denote

$$\mathcal{Q}_I(\mathbf{R}) \triangleq \{(\mathbf{P}_{\text{usa}}, \mathbf{P}_c) : \mathbf{P}_{\text{usa}} \in \bar{\mathcal{O}}_I(\mathbf{P}_c, \mathbf{R})\}. \quad (40)$$

$\mathcal{Q}_I(\mathbf{R})$ is also a convex set.

Thus, we can search for the desired individual usage probability vector by maximizing an objective function of \mathbf{P}_{usa} subject to the power constraint, namely,

$$\max_{(\mathbf{P}_{\text{usa}}, \mathbf{P}_c) \in \mathcal{Q}_I(\mathbf{R})} q_I(\mathbf{P}_{\text{usa}}),$$

$$\text{s.t. } \mathbf{P}_c \leq \bar{\mathbf{P}}. \quad (41)$$

To maximize the individual usage probability with the fairness consideration to each user, the objective function can be chosen to be $q_I(\mathbf{P}_{\text{usa}}) = \sum_{j=1}^J \log(P_{\text{usa},j})$, which is concave [24].

Lemma 3: The feasible region of the optimization problem (41) contains interior points.

Proof: See Appendix C. \blacksquare

As $\mathcal{Q}_I(\mathbf{R})$ is a convex set and $\mathbf{P}_c \leq \bar{\mathbf{P}}$ is a linear constraint, (41) is a convex optimization problem if its objective function is concave. Hence, we will always choose a concave objective function for (41). Furthermore, as the feasible region of (41) has interior points, (41) is equivalent to its Lagrange dual problem. By introducing the variable $\mathbf{v} = \mathbf{P}_{\text{usa}}$, we rewrite (41) as

$$\max_{(\mathbf{P}_{\text{usa}}, \mathbf{P}_c) \in \mathcal{Q}_I(\mathbf{R}), \mathbf{0} \leq \mathbf{v} \leq \mathbf{1}_J} q_I(\mathbf{v}),$$

$$\text{s.t. } \mathbf{P}_c \leq \bar{\mathbf{P}},$$

$$\mathbf{P}_{\text{usa}} = \mathbf{v}. \quad (42)$$

By replacing \mathbf{P}_{usa} and \mathbf{P}_c with $E\{\mathbf{w}(\mathbf{H})\}$ and $E\left\{ \sum_{m=1}^{2^J-1} w(\mathbf{H}, m) u(\mathbf{P}(\mathbf{H}, m)) \right\}$ as well as according to Proposition 2, the Lagrange dual function is expressed as (43) given at the top of this page. The optimal $\mathbf{v}_{\lambda_I, \mu_I}^*$, $\mathbf{P}_{\lambda_I, \mu_I}^*(\mathbf{H}, m)$ and $w_{\lambda_I, \mu_I}^*(\mathbf{H}, m)$ for (43) given Lagrange multipliers λ_I and μ_I can be obtained by solving the following three problems in sequence

$$\max_{\mathbf{0} \leq \mathbf{v} \leq \mathbf{1}_J} q_I(\mathbf{v}) - \mu_I^T \mathbf{v}, \quad (44)$$

$$\min_{\mathbf{P}(\mathbf{H}, m) \geq \mathbf{0}, \forall m} \lambda_I^T u(\mathbf{P}(\mathbf{H}, m)),$$

$$\text{s.t. } \psi(m) \odot \mathbf{R} \in C_{\text{SCMA}}(\mathbf{P}(\mathbf{H}, m), \mathbf{H}), \quad (45)$$

$$\max_{\mathbf{0} \leq w(\mathbf{H}, m) \leq 1, \forall m} \sum_{m=1}^{2^J-1} w(\mathbf{H}, m) (\eta_m - \lambda_I^T u(\mathbf{P}_{\lambda_I, \mu_I}^*(\mathbf{H}, m))),$$

$$\text{s.t. } \sum_{m=0}^{2^J-1} w(\mathbf{H}, m) = 1, \quad (46)$$

where $\eta_m \triangleq \mu_I^T \psi(m)$. The solutions to (44) and (45) can be efficiently obtained by convex optimization tools, such as CVX [34]. Similar to the optimization (19), (46) is a linear optimization problem and has the closed-form solutions. Specifically, denote

$$m^* = \arg \max_{0 \leq m \leq 2^J-1} \eta_m - \lambda_I^T u(\mathbf{P}_{\lambda_I, \mu_I}^*(\mathbf{H}, m)). \quad (47)$$

The solutions to (46) are given by

$$w_{\lambda_I, \mu_I}^*(\mathbf{H}, m) = \begin{cases} 1, & m = m^*, \\ 0 & \forall m \neq m^*. \end{cases} \quad (48)$$

The adaptive algorithm given in (49) at the bottom of this page can be applied to obtain the optimal Lagrange multipliers, where \mathbf{v}_n^I , $\mathbf{P}_n^I(\mathbf{H}[n], m)$ and $w_n^I(\mathbf{H}[n], m)$ denote the solutions to (44)–(46) in the n -th iteration, respectively. The reason that we can use the adaptive algorithm (49) without applying the expectation operations is similar to that for (28). Given the optimal Lagrange multipliers (λ_I^*, μ_I^*) , the optimal individual usage probability

$$\begin{cases} \hat{\lambda}_I[n+1] = \left(\hat{\lambda}_I[n] + \alpha \left(\sum_{m=1}^{2^J-1} w_n^I(\mathbf{H}[n], m) u(\mathbf{P}_n^I(\mathbf{H}[n], m)) - \bar{\mathbf{P}} \right) \right)_\varepsilon^+, \\ \hat{\mu}_I[n+1] = \left(\hat{\mu}_I[n] + \alpha \left(\mathbf{v}_n^I - \sum_{m=1}^{2^J-1} w_n^I(\mathbf{H}[n], m) \psi(m) \right) \right)_\varepsilon^+, \end{cases} \quad (49)$$

Algorithm 1 Adaptive Online Optimal Power Allocation Algorithm

- 1: **Input:** Number of users J , number of power constraints N_P , and power constraint $\bar{\mathbf{P}}$; Lagrange multipliers $\boldsymbol{\lambda} \in \mathbb{R}^{N_P}$ and $\boldsymbol{\mu} \in \mathbb{R}^J$; The set of all the subsets for all the users $\mathcal{K} = \{\mathcal{S}_0, \mathcal{S}_m, 1 \leq m \leq 2^J - 1\}$;
 - 2: **Initialization:** $\boldsymbol{\lambda}[0] = \mathbf{1}_{N_P}$, $\boldsymbol{\mu}[0] = \mathbf{1}_J$, $n = 0$;
 - 3: **while** transmission is ongoing **do**
 - 4: acquire instantaneous channel state $\mathbf{H}[n]$;
 - 5: obtain $\mathbf{v}[n]$ by solving $\max_{\mathbf{0} \leq \mathbf{v} \leq \mathbf{1}_J} q(\mathbf{v}) - \boldsymbol{\mu}^T[n]\mathbf{v}$;
 - 6: obtain $\mathbf{P}^*(\mathbf{H}[n], m)$ for $\mathcal{S}_m \in \mathcal{K}$ by solving

$$\min_{\mathbf{P}(\mathbf{H}[n], m) \geq \mathbf{0}} \boldsymbol{\lambda}^T[n]u(\mathbf{P}(\mathbf{H}[n], m)),$$
 s.t. $\boldsymbol{\psi}(m) \odot \mathbf{R} \in C_{\text{SCMA}}(\mathbf{P}(\mathbf{H}[n], m), \mathbf{H}[n]);$ (50)
 - 7: obtain $\eta_m = \boldsymbol{\mu}^T[n]\boldsymbol{\psi}(m)$, $\mathcal{S}_m \in \mathcal{K}$;
 - 8: obtain $m^* = \arg \max_{\mathcal{S}_m \in \mathcal{K}} \eta_m - \boldsymbol{\lambda}^T[n]u(\mathbf{P}^*(\mathbf{H}[n], m))$;
 - 9: **if** $\eta_{m^*} - \boldsymbol{\lambda}^T[n]u(\mathbf{P}^*(\mathbf{H}[n], m^*)) \geq 0$ **then**
 - 10: $w[n] = 1$;
 - 11: transmit power at this time slot is allocated as $\mathbf{P}[n] = \mathbf{P}^*(\mathbf{H}[n], m^*)$;
 - 12: **else**
 - 13: $w[n] = 0$;
 - 14: transmit power at this time slot is set to $\mathbf{P}[n] = \mathbf{0}$;
 - 15: update the Lagrange multipliers according to

$$\begin{cases} \boldsymbol{\lambda}[n+1] = (\boldsymbol{\lambda}[n] + \alpha(w[n]u(\mathbf{P}[n]) - \bar{\mathbf{P}}))_{\epsilon}^+, \\ \boldsymbol{\mu}[n+1] = (\boldsymbol{\mu}[n] + \alpha(\mathbf{v}[n] - w[n]\boldsymbol{\psi}(m^*)))_{\epsilon}^+; \end{cases}$$
 - 16: $n = n + 1$;
-

vector $\mathbf{P}\mathbf{r}_{\text{usa}}^* = E \left\{ \sum_{m=1}^{2^J-1} w_{\boldsymbol{\lambda}_i^*, \boldsymbol{\mu}_i^*}^*(\mathbf{H}, m)\boldsymbol{\psi}(m) \right\}$ and the corresponding power allocation policy with the form of (35), denoted as $\left\{ \mathbf{P}_{\boldsymbol{\lambda}_i^*, \boldsymbol{\mu}_i^*}^*(\mathbf{H}, m), w_{\boldsymbol{\lambda}_i^*, \boldsymbol{\mu}_i^*}^*(\mathbf{H}, m) \right\}$, can be derived by (45) and (46). If the optimization problem (44) has a unique solution, the property $\mathbf{v}_{\boldsymbol{\lambda}_i^*, \boldsymbol{\mu}_i^*}^* = \mathbf{P}\mathbf{r}_{\text{usa}}^* = E \left\{ \sum_{m=1}^{2^J-1} w_{\boldsymbol{\lambda}_i^*, \boldsymbol{\mu}_i^*}^*(\mathbf{H}, m)\boldsymbol{\psi}(m) \right\}$ is satisfied and, consequently, we can obtain the optimal individual usage probability without applying the expectation operations. Furthermore, the convergence of (49) to the optimal solution $(\boldsymbol{\lambda}_i^*, \boldsymbol{\mu}_i^*)$ is guaranteed.

Based on the above adaptive optimization procedure, we can also design an adaptive online power allocation scheme that calculates the instantaneous power allocation for the current time slot according to the current channel state estimation and the current instantaneous Lagrange multipliers. This adaptive online power allocation scheme is summarized in Algorithm 1, where the index n now represents the time slot index. Explicitly, at the time slot n , line 4 estimates the current channel state $\mathbf{H}[n]$, line 5 finds the optimal instantaneous individual outage probability vector given the current Lagrange multipliers, and line 6 determines the power allocation functions for all the user subsets given the current channel state and

current Lagrange multipliers, while lines 7 to 14 calculates the optimal power allocation scheme for the current time slot. The Lagrange multipliers are then updated in line 15, and the adaptive online algorithm is ready for the operations of the next time slot.

A similar adaptive online power allocation scheme for the optimized common outage probability can be derived as a special case of Algorithm 1 with the following modifications. Specifically, in this case, $\mathcal{K} = \{\{1, 2, \dots, J\}\}$, the power allocation function becomes $\mathbf{P}(\mathbf{H})$, $\boldsymbol{\mu}$ becomes one-dimensional, i.e., μ , and \mathbf{v} also becomes one-dimensional, i.e., v , while $\boldsymbol{\psi}(m)$ also is one-dimensional and is fixed to 1, and the operator \odot in (50) becomes the multiplication. Moreover, since there is only a single η , lines 7 and 8 are no longer needed, while line 9 becomes: **if** $\mu[n] - \boldsymbol{\lambda}^T[n]u(\mathbf{P}^*(\mathbf{H}[n])) \geq 0$ **then**.

VII. SIMULATION RESULTS

1) *Two-User System:* First, we consider a two-user ($J = 2$) system with $K = 4$ and $N_1 = N_2 = 2$. The resource assignment matrix is given by

$$\mathbf{F}_{4,2} = \begin{bmatrix} 1 & 1 \\ 1 & 0 \\ 0 & 1 \\ 0 & 0 \end{bmatrix}. \quad (51)$$

Two types of linear power constraints are considered, namely, the individual power constraint $u(\mathbf{P}) = \mathbf{P}^T \mathbf{1}_K \in \mathbb{R}^2$, and the sum power constraint $u(\mathbf{P}) = \mathbf{1}_K^T \mathbf{P} \mathbf{1}_J \in \mathbb{R}$. Considering the power allocation functions that satisfy a power constraint $u(\mathbf{P}) \leq \bar{\mathbf{P}}$, we can define the feasible region of (10) with respect to \mathbf{R} as the feasible capacity region under the power constraint $\bar{\mathbf{P}}$

$$C(\bar{\mathbf{P}}, \mathbf{H}) = \bigcup_{\mathbf{P}: u(\mathbf{P}) \leq \bar{\mathbf{P}}} C_{\text{SCMA}}(\mathbf{P}, \mathbf{H}). \quad (52)$$

That is, the feasible capacity region is the union of all the capacity regions whose power allocation functions meet the given power constraint. Clearly, the feasible capacity region is convex.

For the instantaneous channel state \mathbf{H} given in (53), Fig. 3 compares the SCMA feasible capacity region (52) under the equal individual power constraint of $\bar{\mathbf{P}} = [\frac{1}{2} \ \frac{1}{2}]^T$ with the SCMA capacity regions (5) with the two power allocation functions \mathbf{P}_1 and \mathbf{P}_2 given in (53)

$$\mathbf{P}_1 = \begin{bmatrix} \frac{1}{4} & \frac{1}{4} \\ \frac{1}{4} & 0 \\ 0 & \frac{1}{4} \\ 0 & 0 \end{bmatrix}, \quad \mathbf{P}_2 = \begin{bmatrix} \frac{1}{4} & \frac{3}{8} \\ \frac{1}{4} & 0 \\ 0 & \frac{1}{8} \\ 0 & 0 \end{bmatrix}, \quad \mathbf{H} = \begin{bmatrix} 1 & 1 \\ 1 & 1 \\ 1 & 1 \\ 1 & 1 \end{bmatrix}. \quad (53)$$

As can be observed from Fig. 3, the SCMA capacity regions with the power allocation functions \mathbf{P}_1 and \mathbf{P}_2 are the subsets of the SCMA feasible capacity region under the equal individual power constraint $\bar{\mathbf{P}} = [\frac{1}{2} \ \frac{1}{2}]^T$. The capacity region of the LDS system with the power allocation function \mathbf{P}_1 is also

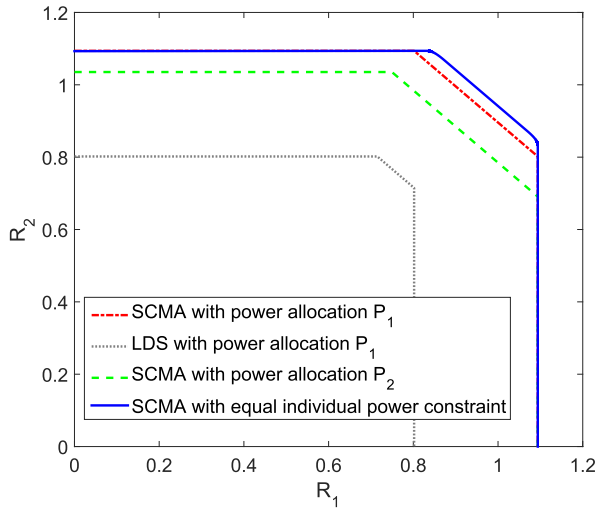


Fig. 3. The SCMA capacity regions under the power allocation functions P_1 and P_2 and the SCMA feasible capacity region under the equal individual power constraint as well as the LDS capacity region under P_1 . The SCMA resource assignment matrix is $F_{4,2}$ of (51). The channel state H as well as P_1 and P_2 are given in (53). The noise power is $\sigma_n^2 = -10$ dBW.

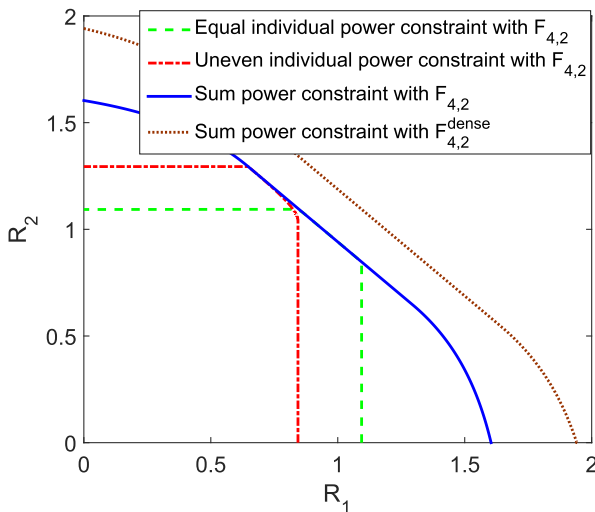


Fig. 4. The feasible capacity regions under various power constraints for the two-user SCMA systems with $F_{4,2}$ and $F_{4,2}^{dense}$, given the noise power $\sigma_n^2 = -10$ dBW.

plotted in Fig. 3 given the same channel state H . Clearly, the LDS capacity region is a subset of the SCMA capacity region under the same power allocation function and channel state, which is consistent with the analysis of Section III.

The feasible capacity regions $C(\bar{P}, H)$ with the equal individual power constraint $\bar{P}_1 = [\frac{1}{2} \ \frac{1}{2}]^T$, the uneven individual power constraint $\bar{P}_2 = [\frac{1}{3} \ \frac{2}{3}]^T$, and the sum power constraint $\bar{P} = 1$ are shown in Fig. 4 for the SCMA system with $F_{4,2}$ of (51) and the channel state H given in (53). It can be seen that the feasible capacity region under the sum power constraint is larger than the feasible capacity region under an individual power constraint, because the sum power constraint $\bar{P} = 1$ is looser than an individual power constraint. In Fig. 4, we also plot the feasible capacity region with the sum power

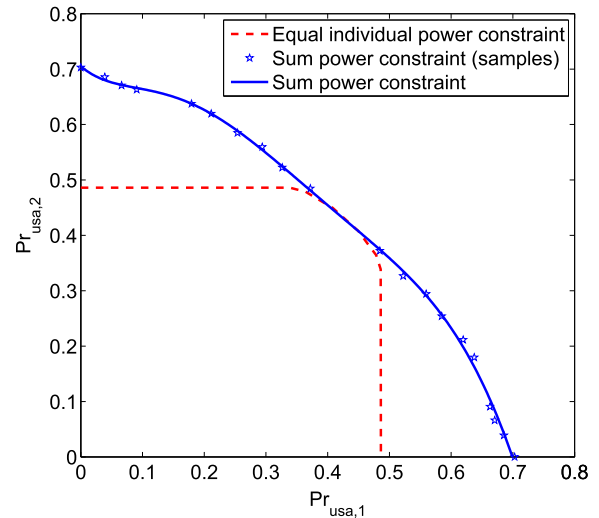


Fig. 5. The individual usage probability regions under the equal individual power constraint and the sum power constraint for the two-user SCMA system with $F_{4,2}$ given the noise power $\sigma_n^2 = -10$ dBW.

constraint $\bar{P} = 1$ for the SCMA system with a denser resource assignment matrix $F_{4,2}^{dense}$

$$F_{4,2}^{dense} = \begin{bmatrix} 1 & 1 \\ 1 & 0 \\ 0 & 1 \\ 1 & 1 \end{bmatrix}. \quad (54)$$

Clearly, the feasible capacity region under the sparser $F_{4,2}$ is smaller than that under $F_{4,2}^{dense}$. This confirms our analysis given in Sections II and III.

The individual usage probability region for the two-user SCMA system with $F_{4,2}$ is then calculated. Rayleigh fading channels with unitary average power at each resource are considered, the pathloss losses are set to one for the two users, and the rate vector is set to $R = [2 \ 2]^T$. We choose $q_I(v) = a^T v$, where $a \in \mathbb{R}^J$, $a > 0$ and $\|a\| = 1$. By rotating a , we can obtain the boundary of the individual usage probability region. Specifically, we calculate sufficient samples on the boundary by the adaptive procedure of Section VI. By smoothing these samples to yield a smoothed boundary, we obtain the individual usage probability region. This is illustrated in Fig. 5 for the individual usage probability region under the sum power constraint of $\bar{P} = 1$. Clearly, the samples are not strictly on the smoothed boundary, due to the fluctuations of the adaptive algorithm utilized in calculating these samples. The individual usage probability region under the equal individual power constraint $\bar{P} = [\frac{1}{2} \ \frac{1}{2}]^T$ depicted in Fig. 5 is similarly obtained, which is a subset of the individual usage probability region under the sum power constraint.

Fig. 6 compares the individual usage probability regions of the PD-NOMA and the SCMA under sum power constraint $\bar{P} = 1$, where the same resource assignment matrix $F_{4,2}$ (51) is adopted by the two systems, the path losses for the two users are set to $3/\sqrt{10}$ and $1/\sqrt{10}$, respectively, and the rate vector is set to $R = [2 \ 0.5]^T$. It is seen that the individual

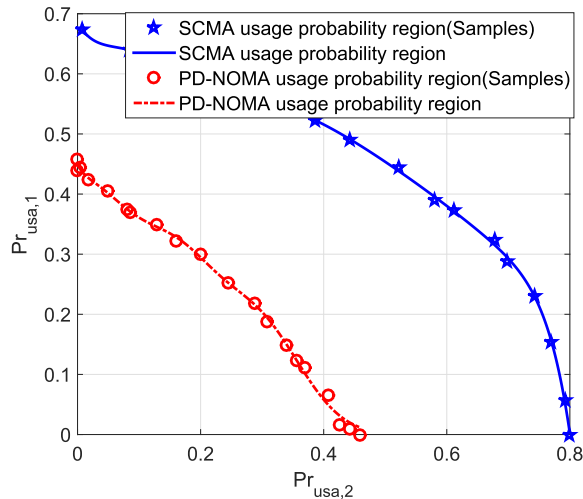


Fig. 6. Comparison of the individual usage probability regions for the two-user SCMA and PD-NOMA under the equal sum power constraint given the noise power $\sigma_n^2 = -10$ dBW.

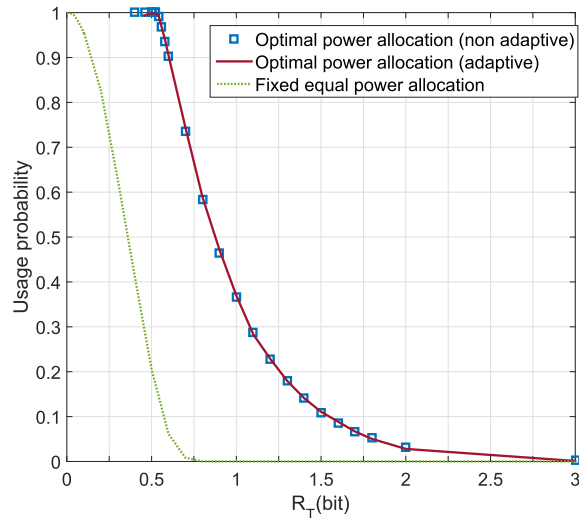


Fig. 7. Comparison of the common usage probabilities as the functions of the user rate R_T obtained by the optimal power allocation under the sum power constraint and by the fixed equal power allocation for the six-user SCMA system with the noise power $\sigma_n^2 = -13$ dBW.

usage probability region of the SCMA is larger than that of the PD-NOMA.

2) *Six-User System*: Next, we set $K = 4$, $J = 6$, and $N_j = 2$ for $1 \leq j \leq 6$, which is the system used in [4]. The resource assignment matrix $F_{4,6}$ given in (1) is adopted, the noise power is set to $\sigma_n^2 = -13$ dBW, and Rayleigh fading channels with unitary average power at each resource are considered, while the path loss is set to one for every user. To evaluate the maximum common usage probability, we set $q_C(v) = 3v - v^2$, which is monotonically increasing and strictly concave for $0 \leq v \leq 1$. Assume that the rate requirements for all the users are the same, namely, $R_j = R_T$ for $1 \leq j \leq 6$. The maximum common usage probabilities of the required data rate vector $\mathbf{R} = R_T \mathbf{1}_J$ under the sum power constraint $u(\mathbf{P}) = \mathbf{1}_K^T \mathbf{P} \mathbf{1}_J \leq 1$ W, obtained by both the non-adaptive iterative algorithm and its adaptive version given in Section V, are plotted in Fig. 7, where the step size

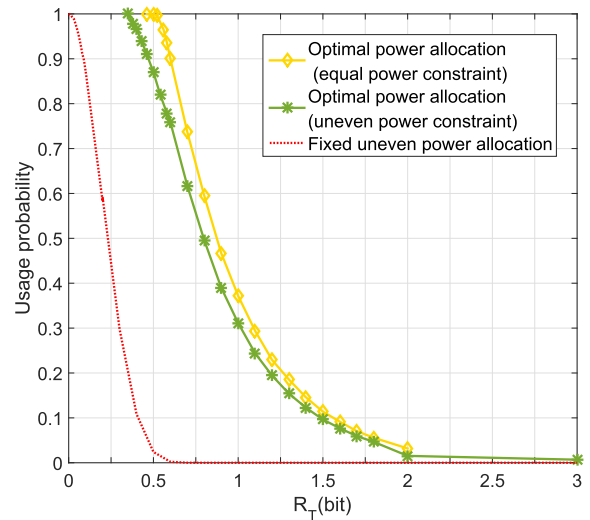


Fig. 8. Comparison of the common usage probabilities as the functions of the user rate R_T obtained by the optimal power allocation under the equal individual power constraint and the unequal individual power constraint as well as by the fixed uneven power allocation for the six-user SCMA system with the noise power $\sigma_n^2 = -13$ dBW.

is set to $\alpha = 0.001$. Observe that the performance of the low-complexity adaptive algorithm is indistinguishable from that of the high-complexity non-adaptive algorithm. To further demonstrate the effectiveness of our proposed optimization approach, the common usage probability achieved by the fixed equal power allocation scheme, which distributes power equally among the users according to $\mathbf{P}_{\text{equal}}(\mathbf{H}) = \frac{1}{12} \mathbf{F}_{4,6}$, is also plotted in Fig. 7. It can be seen from Fig. 7 that the optimized power allocation scheme outperforms the fixed equal power allocation scheme dramatically.

Fig. 8 compares the maximum common usage probabilities of the data rate vector $\mathbf{R} = R_T \mathbf{1}_J$ obtained under the equal individual power constraint $u(\mathbf{P}) \leq \frac{1}{6} \mathbf{1}_J$ and the uneven individual power constraint $u(\mathbf{P}) \leq [\frac{1}{15} \frac{1}{15} \frac{1}{15} \frac{1}{15} \frac{4}{15} \frac{4}{15}]^T$. Since the Rayleigh fading channels with unitary power at each resource are assumed, higher common usage probability can be achieved under the equal individual power constraint than under the uneven individual power constraint. In Fig. 8, the common usage probability attained under the fixed uneven power allocation function of

$$\mathbf{P}_{\text{uneven}}(\mathbf{H}) = \frac{1}{30} \begin{bmatrix} 1 & 1 & 1 & 0 & 0 & 0 \\ 1 & 0 & 0 & 4 & 4 & 0 \\ 0 & 1 & 0 & 4 & 0 & 4 \\ 0 & 0 & 1 & 0 & 4 & 4 \end{bmatrix}, \quad (55)$$

is also depicted. It can be seen that the common usage probability with the fixed allocation function (55) is significantly lower than the maximum common usage probability obtained by the optimal power allocation under the equivalent uneven power constraint of $[\frac{1}{15} \frac{1}{15} \frac{1}{15} \frac{4}{15} \frac{4}{15} \frac{4}{15}]^T$.

Fig. 9 illustrates the convergence of the adaptive algorithm for solving the maximum common usage probability at $R_T = 0.9$ bit, where the same simulation system as in Fig. 7 is utilized. It can be seen from Fig. 9 that $\hat{\Lambda}[n]$ converges for sufficiently large n . Also the fluctuations of $\hat{\Lambda}[n]$ owing to

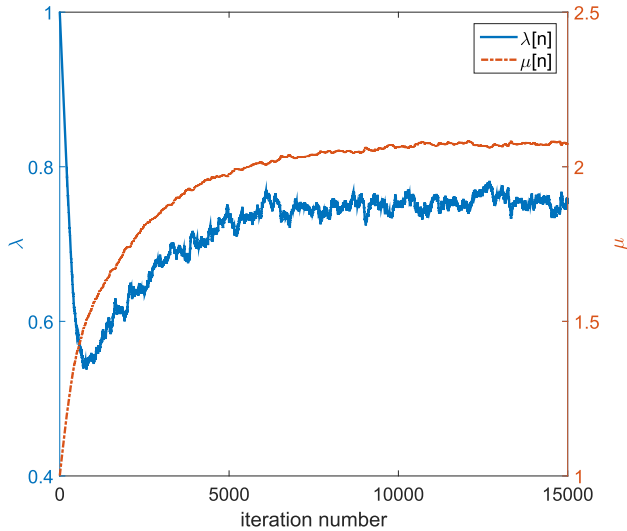


Fig. 9. Convergence of the adaptive algorithm with step size $\alpha = 0.001$ for maximizing the common usage probability under the sum power constraint for the six-user SCMA system with the noise power $\sigma_n^2 = -13$ dBW.

using the instantaneous channel state $\mathbf{H}[n]$ are relatively small and, consequently, the fluctuations related to the optimized common usage probability is negligible, as can be observed from Fig. 7. Thus, the accuracy of the proposed adaptive algorithm is guaranteed.

Lastly, we compare the average BER performance of the practical SCMA systems with the resource assignment matrix $\mathbf{F}_{4,6}$ and the MPA detection under Rayleigh fading channels, which implement a fixed power allocation and the optimal power allocation attained by the proposed power allocation algorithm given in Section V, respectively. We assume $N_{B,j} = N_B$, $1 \leq j \leq J$, and hence the codebook size for each user is equal to 2^{N_B} . We consider two practical codebook designs. In the first case, we have $N_B = 2$ bits, and the codebook or constellation is given by (7), while in the second case, $N_B = 1$ bit and the codebook is designed as

$$\left\{ \begin{bmatrix} 1 \\ -j \end{bmatrix}, \begin{bmatrix} -1 \\ j \end{bmatrix} \right\}. \quad (56)$$

Note that the design (56) cannot achieve diagonal $E\{\mathbf{c}_j \mathbf{c}_j^H\}$. For the optimization associated with the proposed power allocation algorithm, the individual power constraint of $\mathbf{P} = \mathbf{1}_J$ is used. The system's signal to noise ratio (SNR) is defined as $\text{SNR} = \mathbf{1}_J^T \mathbf{P} / J \sigma_n^2$. From Fig. 10, it is seen that our proposed optimal power allocation policy significantly enhances the BER performance. At the BER level of 10^{-3} , the system implementing our optimal power allocation attains more than 3 dB SNR gain over the same system with the non-optimal power allocation.

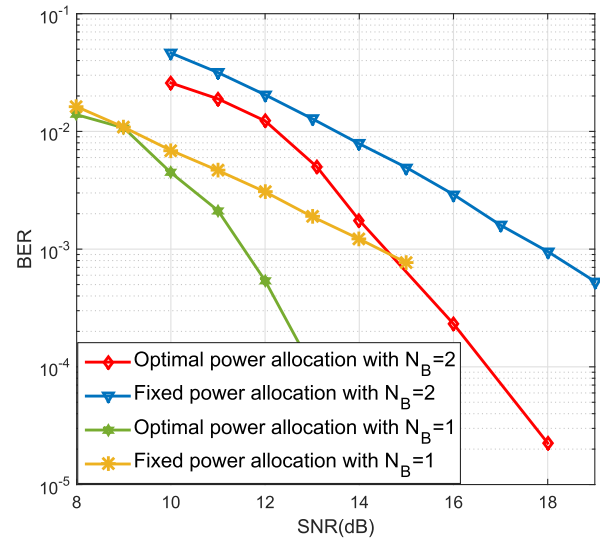


Fig. 10. Comparison of the BER performance averaged over the six users achieved with and without the optimal power allocation for the six-user SCMA systems with the practical codebook designs of (7) and (56).

VIII. FUTURE WORK

A. Multi-Cell System

We outline how to extend our work for the single-cell scenario to the multi-cell scenario with inter-cell interference. Consider the system with N_{cell} cells. Let $\mathbf{P}^{\text{mul}} = \{\mathbf{P}^l = [p_{k,j}^l]\}_{l=1}^{N_{\text{cell}}}$ be the set of all the power allocation matrices for all the users from the N_{cell} cells, and denote the resource assignment matrix of the l th cell as $\mathbf{F}^l = [f_{k,j}^l]$. Further let $\mathbf{R}^{\text{mul}} = \{\mathbf{R}^l = [R_j^l]\}_{l=1}^{N_{\text{cell}}}$ be the set of all the data rate vectors of all the cells, and denote $\mathbf{H}^{\text{mul}} = \{\mathbf{H}^l\}_{l=1}^{N_{\text{cell}}}$ as the set of all the channel states of all the cells. Then the capacity region can be expressed as (57) given at the bottom of this page, where $\mathcal{S}^l \subset \{1, \dots, J^l\}$ and J^l is the number of users in the l th cell, $h_{k,j}^l$ is the channel gain of the j th user's signal at the k th orthogonal resource for BS l , and $p_{k,j}^l$ is the signal power of the j th user in the l th cell at the k th orthogonal resource, and γ_k^l represents the inter-cell interference which is calculated as $\gamma_k^l = \sum_{q=1, q \neq l}^{N_{\text{cell}}} \sum_{u=1}^{J^q} |h_{k,u}^q|^2 p_{k,u}^q f_{k,u}^q$. Again, $p_{k,j}^l$ is nonzero only if $f_{k,j}^l = 1$.

With the above SCMA capacity region, denote $\mathbf{Pr}_{\text{usa}}^{\text{mul}} = [\mathbf{Pr}_{\text{usa}}^1 \cdots \mathbf{Pr}_{\text{usa}}^{N_{\text{cell}}}]$ as the usage probability matrix for all the cells, and let $\mathbf{P}^{\text{mul}} = \{\mathbf{P}^l\}_{l=1}^{N_{\text{cell}}}$ be the power constraints for all the cells. Then the individual usage probability region for the multi-cell scenario can be expressed as (58), as shown at the top of the next page.

As expected, extending the single-cell model to the multi-cell model is rather straightforward. However, the capacity

$$\mathcal{C}_{\text{SCMA}}^{\text{mul}}(\mathbf{P}^{\text{mul}}, \mathbf{H}^{\text{mul}}) = \left\{ \mathbf{R}^{\text{mul}} : \sum_{j \in \mathcal{S}^l} R_j^l \leq \sum_{k=1}^K \log \left(1 + \frac{1}{\sigma_n^2 + \gamma_k^l} \sum_{j \in \mathcal{S}^l} |h_{k,j}^l|^2 p_{k,j}^l f_{k,j}^l \right) \right\}, \quad (57)$$

$$\bar{O}_I^{\text{mul}}(\bar{\mathbf{P}}^{\text{mul}}, \mathbf{R}^{\text{mul}}) = \bigcup_{\{w^l(\mathbf{H}^{\text{mul}}, m^l)\}, \{\mathbf{P}^l(\mathbf{H}^{\text{mul}}, m^l) \geq \mathbf{0}\}, \forall m^l} E\{\mathbf{w}^{\text{mul}}(\mathbf{H}^{\text{mul}})\}, \quad (58)$$

where

$$\mathbf{w}^{\text{mul}}(\mathbf{H}^{\text{mul}}) \triangleq \left[\sum_{m=0}^{2^{J^1}-1} w^1(\mathbf{H}^{\text{mul}}, m) \psi^1(m) \cdots \sum_{m=0}^{2^{J^{N_{\text{cell}}}}-1} w^{N_{\text{cell}}}(\mathbf{H}^{\text{mul}}, m) \psi^{N_{\text{cell}}}(m) \right], \quad (59)$$

$$E \left\{ \sum_{m=1}^{2^{J^l}-1} w^l(\mathbf{H}^{\text{mul}}, m) u(\mathbf{P}^l(\mathbf{H}^{\text{mul}}, m)) \right\} \leq \bar{\mathbf{P}}^l, \quad (60)$$

$$\{\psi^l(m^l) \odot \mathbf{R}^l\} \in C_{\text{SCMA}}^{\text{mul}}(\mathbf{P}^{\text{mul}}(\mathbf{H}^{\text{mul}}, m^l), \mathbf{H}^{\text{mul}}), \forall \mathbf{H}^{\text{mul}}, \exists m^l : w^l(\mathbf{H}^{\text{mul}}, m^l) > 0. \quad (61)$$

region analysis, the common outage probability optimization and the individual outage probability optimization are very challenging. This is because owing to inter-cell interference, all the associated optimization problems are nonconvex and, therefore, the optimal results are not assured. In particular, we can apply our approaches to solve these nonconvex optimization problems but we can only guarantee local optimal results. We will further analyze the solutions to the optimization problem for the outage probability region under multi-cell scenarios in our future work, with the aim of developing effective optimal solutions.

B. Joint Codebook and Power Allocation

In this paper, the outage probability region given the codebook allocation policy \mathbf{F} is calculated. More specifically, calculating the boundary of the outage probability region is formulated as an optimization problem for the power allocation policy, which is efficiently solved via its Lagrangian dual problem. It is worth recapping that given the codebook assignment matrix \mathbf{F} , the associated optimization problem (23) (or (43)) is convex, and we guarantee to obtain the global optimal solution.

It is possible to extend our current work and to formulate the associated optimization problem for joint codebook and power allocation to select the optimal \mathbf{F}_{opt} from the set of all the possible codebook assignment matrices \mathcal{F} that minimizes the outage probability. Without loss of generality, let us set $N_j = N$ for $1 \leq j \leq J$. Also note that no two columns of a resource allocation matrix \mathbf{F} can be identical. Then the number of all the possible codebook assignment matrices or the size of \mathcal{F} is given by

$$|\mathcal{F}| = \prod_{j=1}^J \left(\binom{K}{N} - (j-1) \right). \quad (62)$$

The optimal codebook assignment matrix \mathbf{F}_{opt} in theory can be obtained by the exhaustive search which solves the optimization problem (23) (or (43)) for every $\mathbf{F} \in \mathcal{F}$.

Because the size of \mathcal{F} is typically very large, the computational complexity of the exhaustive search may become practically unaffordable. An alternative is to simply apply some suboptimal search strategy to attain a suboptimal codebook assignment matrix \mathbf{F} . Since our work is about the analysis

and calculation of the outage probability region, we need to investigate more effective search methods to solve this joint optimal codebook and power allocation problem, which can guarantee that the solution obtained is the true optimal solution, while imposing practically affordable complexity. This will be studied in future work.

IX. CONCLUSIONS

We have derived the expression of the capacity region for uplink SCMA systems based on the characteristics of SCMA multi-dimensional codebooks. With the aid of this capacity region expression, the common outage and individual outage probability regions given required data rate vector have been provided. Moreover, the tractable expressions of these two outage probability regions have been formulated for ease of computation. Optimizing the common outage probability and individual outage probability have been formulated as convex optimization problems, which are equivalent to their Lagrangian dual problems and can be solved using the iterative descent method. To reduce computational complexity, an adaptive algorithm has been developed based on the instantaneous channel state to optimize the common outage and individual outage probabilities. Both the theoretical analysis and simulation results have demonstrated that this low-complexity adaptive algorithm is capable of converging to the same optimal solution provided by its high-complexity non-adaptive counterpart.

APPENDIX

A. Proof of Lemma 1

Proof: It is reasonable to assume that $\bar{\mathbf{P}} > \mathbf{0}$. We first prove that for any power constraint $\mathbf{P}_c > \mathbf{0}$, $\bar{O}_C(\mathbf{P}_c, \mathbf{R})$ has interior points.

For any channel state \mathbf{H}_0 , we can define the probability $Pr_t(\mathbf{H}_0) \triangleq \Pr[|\mathbf{H}| \geq |\mathbf{H}_0|]$ according to the channel state's continuous CDF. Choose a channel state \mathbf{H}_0 satisfying $Pr_t(\mathbf{H}_0) > 0$. For this channel state, we can always find a power allocation function \mathbf{P}_0 which is sufficiently large such that $\mathbf{R} \in C_{\text{SCMA}}(\mathbf{P}_0, \mathbf{H}_0)$. Then for the channel states \mathbf{H} that satisfy $|\mathbf{H}| \geq |\mathbf{H}_0|$, it is apparent that $\mathbf{R} \in C_{\text{SCMA}}(\mathbf{P}_0, \mathbf{H})$ because according to the expression of SCMA

capacity region (5), C_{SCMA} expands as the magnitudes of the elements of channel state increases.

Since $\mathbf{P}_c > \mathbf{0}$, there exists a small positive number $0 < \delta \leq 1$ that satisfies $\delta \cdot Pr_t(\mathbf{H}_0) \cdot u(\mathbf{P}_0) \leq \mathbf{P}_c$. Thus, we can design a power allocation policy that allocates power function \mathbf{P}_0 only to those channel states which fulfill $|\mathbf{H}| \geq |\mathbf{H}_0|$, while no power is transmitted for other channel states, where the percentage of the activated channel states is equal to $\delta \cdot Pr_t(\mathbf{H}_0)$. Under this policy, the usage probability is equal to $\delta \cdot Pr_t(\mathbf{H}_0) > 0$ and the average power $\delta \cdot Pr_t(\mathbf{H}_0) \cdot \mathbf{P}_0$ satisfies $\delta \cdot Pr_t(\mathbf{H}_0) \cdot \mathbf{P}_0 \leq \mathbf{P}_c$. Therefore, according to the definition of common usage probability region, the segment $[0, \delta \cdot Pr_t(\mathbf{H}_0)]$ is within $\bar{\mathcal{O}}_C(\mathbf{P}_c, \mathbf{R})$. Thus, for the power constraint $\mathbf{P}_c > \mathbf{0}$, $\bar{\mathcal{O}}_C(\mathbf{P}_c, \mathbf{R})$ has interior points.

Next for any power allocation policy $\mathbf{P}^{\text{rand}}(\mathbf{H})$ that satisfies $E\{u(\mathbf{P}^{\text{rand}}(\mathbf{H}))\} \leq \mathbf{P}_c$, it is apparent that $E\{u(\mathbf{P}^{\text{rand}}(\mathbf{H}))\} \leq \mathbf{P}_c + \Theta$ always holds, where Θ has the same size as \mathbf{P}_c and all the its elements are positive. Thus, $\bar{\mathcal{O}}_C(\mathbf{P}_c, \mathbf{R}) \subseteq \bar{\mathcal{O}}_C(\mathbf{P}_c + \Theta, \mathbf{R})$.

Suppose that $\mathbf{0} < \mathbf{P}_{\text{int}} < \bar{\mathbf{P}}$. According to the above statement, we can choose an interior point Pr_{int} of $\bar{\mathcal{O}}_C(\mathbf{P}_{\text{int}}, \mathbf{R})$ so that $\{(Pr_{\text{usa}}, \mathbf{P}_c) : 0 \leq Pr_{\text{usa}} \leq Pr_{\text{int}}, \mathbf{P}_{\text{int}} \leq \mathbf{P}_c \leq \bar{\mathbf{P}}\}$ is in the feasible region of (15). Therefore, the feasible region of (15) has interior points. ■

B. Proof of Lemma 2

Proof: The descent directions of (28) and (27) can be denoted respectively by

$$\hat{\phi}(\Lambda, \mathbf{H}[n]) = \begin{bmatrix} w_n^C(\mathbf{H}[n])u(\mathbf{P}_n^C(\mathbf{H}[n])) - \bar{\mathbf{P}}} \\ v_n^C - w_n^C(\mathbf{H}[n]) \end{bmatrix}, \quad (63)$$

$$\phi(\Lambda) = E \left\{ \hat{\phi}(\Lambda, \mathbf{H}[n]) \right\}. \quad (64)$$

To prove (31), it is sufficient to verify that the following five conditions hold [36].

- (C1) The expectation of $\hat{\phi}(\Lambda, \mathbf{H}[n])$, i.e., $\phi(\Lambda)$, is time-invariant.
- (C2) For the algorithm (27), $\phi(\Lambda)$ is bounded by a ball. That is, if $\|\Lambda\| \leq B_\Lambda$, we have $\|\phi(\Lambda)\| \leq B_\phi$.
- (C3) Initialization $\Lambda[0]$ is sufficiently small so that $\Lambda[n]$ of the algorithm (27) remains bounded for $n \in \{1, 2, \dots, T/\alpha\}$, i.e., $\|\Lambda[n]\| \leq B_\Lambda$ for $n \in \{1, 2, \dots, T/\alpha\}$.
- (C4) $\hat{\phi}(\Lambda, \mathbf{H}[n])$ obeys the stochastic Lipschitz condition

$$\left\| \hat{\phi}(\Lambda, \mathbf{H}[n]) - \hat{\phi}(\Lambda', \mathbf{H}[n]) \right\| \leq L_\phi[n] \|\Lambda - \Lambda'\|, \quad \forall \|\Lambda\|, \|\Lambda'\| \leq B_\Lambda, \quad (65)$$

where $L_\phi[n]$ is a random sequence satisfying

$$N^{-1} \sum_{n=1}^N L_\phi[n] \rightarrow L_\phi \text{ with probability 1} \\ \text{as } N \rightarrow \infty. \quad (66)$$

- (C5) The deviation $\Delta(N, \Lambda) \triangleq \sum_{n=1}^N (\hat{\phi}(\Lambda, \mathbf{H}[n]) - \phi(\Lambda))$ is stochastic Lipschitz, i.e.,
- (C5.1) $\|\Delta(N, \Lambda)\| \leq B_\Delta[N]$,

$$(C5.2) \|\Delta(N, \Lambda) - \Delta(N, \Lambda')\| \leq L_\Delta[N] \|\Lambda - \Lambda'\|, \\ \forall \|\Lambda\|, \|\Lambda'\| \leq B_\Lambda, \text{ whereas } N \rightarrow \infty, \\ B_\Delta[N]/N \rightarrow 0 \text{ and } L_\Delta[N]/N \rightarrow 0 \text{ with} \\ \text{probability 1.}$$

Conditions (C1)–(C3) hold for the ergodic fading channel with a continuous CDF. (C4) and (C5) can be verified with the similar arguments as the proof given in [24], assuming that the objective function $q_C(\cdot)$ in (22) is strictly concave and the fading channel has a continuous CDF. Thus, (C1)–(C5) hold. According to [36], we can obtain the expression of $c_T(\alpha)$ which is related to the Lipschitz coefficients in (C4) and (C5). Moreover, $c_T(\alpha)$ includes a polynomial function $f(\alpha)$ with $f(0) = 0$ as its factor. Thus, $c_T(\alpha) \rightarrow 0$ as $\alpha \rightarrow 0$. This completes the proof. ■

C. Proof of Lemma 3

Proof: According to the definitions of common and individual outage (usage) probabilities, the common outage probability can be viewed as a special case of the individual outage probability. Specifically, for a fixed data rate \mathbf{R} , we consider a data rate allocation function $\mathbf{R}(\mathbf{P}, \mathbf{H})$: if $\mathbf{R} \in C_{\text{SCMA}}(\mathbf{P}, \mathbf{H})$, $\mathbf{R}(\mathbf{P}, \mathbf{H}) = \mathbf{R}$; otherwise, $\mathbf{R}(\mathbf{P}, \mathbf{H}) = \mathbf{0}$. Under this scenario, the individual usage probability is calculated as $\mathbf{Pr}_{\text{usa}} = \Pr[\mathbf{R} \in C_{\text{SCMA}}(\mathbf{H}, \mathbf{P})] \mathbf{1}_J = Pr_{\text{usa}} \mathbf{1}_J$.

Thus, for any power constraint $\mathbf{P}_c > \mathbf{0}$, considering the power allocation policy applied in the proof of Lemma 1 and the above mentioned data rate allocation function $\mathbf{R}(\mathbf{P}, \mathbf{H})$, the individual usage probability vector is calculated as $\delta \cdot Pr_t(\mathbf{H}_0) \mathbf{1}_J > \mathbf{0}$ and the power constraint is satisfied. Hence, $\delta \cdot Pr_t(\mathbf{H}_0) \mathbf{1}_J \in \bar{\mathcal{O}}_I(\mathbf{P}_c, \mathbf{R})$. According to the definition of the individual usage probability region, $\{\mathbf{Pr}_{\text{usa}} : 0 \leq Pr_{\text{usa},j} \leq \delta \cdot Pr_t(\mathbf{H}_0), j \in \{1, 2, \dots, J\}\} \subseteq \bar{\mathcal{O}}_I(\mathbf{P}_c, \mathbf{R})$. Therefore, the individual usage probability region $\bar{\mathcal{O}}_I(\mathbf{P}_c, \mathbf{R})$ has interior points.

We can use the similar statement in the proof of Lemma 1 to verify that $\bar{\mathcal{O}}_I(\mathbf{P}_c, \mathbf{R}) \subseteq \bar{\mathcal{O}}_I(\mathbf{P}_c + \Theta, \mathbf{R})$, where $\Theta > \mathbf{0}$.

Suppose that $\mathbf{0} < \mathbf{P}_{\text{int}} < \bar{\mathbf{P}}$. According to the above statement, we can choose an interior point Pr_{int} of $\bar{\mathcal{O}}_I(\mathbf{P}_{\text{int}}, \mathbf{R})$ such that $\{(Pr_{\text{usa}}, \mathbf{P}_c) : \mathbf{0} \leq \mathbf{Pr}_{\text{usa}} \leq \mathbf{Pr}_{\text{int}}, \mathbf{P}_{\text{int}} \leq \mathbf{P}_c \leq \bar{\mathbf{P}}\}$ is in the feasible region of (42). Therefore, the feasible region of (42) has interior points. ■

REFERENCES

- [1] F. Boccardi, R. W. Heath, A. Lozano, T. L. Marzetta, and P. Popovski, "Five disruptive technology directions for 5G," *IEEE Commun. Mag.*, vol. 52, no. 2, pp. 74–80, Feb. 2014.
- [2] Q. Wang, R. Zhang, L.-L. Yang, and L. Hanzo, "Non-orthogonal multiple access: A unified perspective," *IEEE Wireless Commun.*, vol. 25, no. 2, pp. 10–16, Apr. 2018.
- [3] Z. Ding, X. Lei, G. K. Karagiannis, R. Schober, J. Yuan, and V. Bhargava, "A survey on non-orthogonal multiple access for 5G networks: Research challenges and future trends," *IEEE J. Sel. Areas Commun.*, vol. 35, no. 10, pp. 2181–2195, Oct. 2017.
- [4] H. Nikopour and H. Baligh, "Sparse code multiple access," in *Proc. PIMRC*, London, U.K., Sep. 2013, pp. 332–336.
- [5] J. Zhang *et al.*, "PoC of SCMA-based uplink grant-free transmission in UCNC for 5G," *IEEE J. Sel. Areas Commun.*, vol. 35, no. 6, pp. 1353–1362, Jun. 2017.

- [6] L. Lei, C. Yan, G. Wenting, Y. Huilian, W. Yiqun, and X. Shuangshuang, "Prototype for 5G new air interface technology SCMA and performance evaluation," *China Commun.*, vol. 12, no. 9, pp. 38–48, Sep. 2015.
- [7] T. Guess, "CDMA with power control and sequence design: The capacity region with and without multidimensional signaling," *IEEE Trans. Inf. Theory*, vol. 50, no. 11, pp. 2604–2619, Nov. 2004.
- [8] O. Kaya and S. Ulukus, "Achieving the capacity region boundary of fading CDMA channels via generalized iterative waterfilling," *IEEE Trans. Wireless Commun.*, vol. 5, no. 11, pp. 3215–3223, Nov. 2006.
- [9] M. Yoshida and T. Tanaka, "Analysis of sparsely-spread CDMA via statistical mechanics," in *Proc. ISIT*, Seattle, WA, USA, Jul. 2006, pp. 2378–2382.
- [10] R. Hoshyar, F. P. Wathan, and R. Tafazolli, "Novel low-density signature for synchronous CDMA systems over AWGN channel," *IEEE Trans. Signal Process.*, vol. 56, no. 4, pp. 1616–1626, Apr. 2008.
- [11] J. Choi, "Low density spreading for multicarrier systems," in *Proc. ISSSTA*, Sydney, NSW, Australia, Aug./Sep. 2004, pp. 575–578.
- [12] M. Taherzadeh, H. Nikopour, A. Bayesteh, and H. Baligh, "SCMA codebook design," in *Proc. VTC Fall*, Vancouver, BC, Canada, Sep. 2014, pp. 1–5.
- [13] L. Yu, X. Lei, P. Fan, and D. Chen, "An optimized design of SCMA codebook based on star-QAM signaling constellations," in *Proc. WCSP*, Nanjing, China, Oct. 2015, pp. 1–5.
- [14] J. Peng, W. Chen, B. Bai, X. Guo, and C. Sun, "Joint optimization of constellation with mapping matrix for SCMA codebook design," *IEEE Signal Process. Lett.*, vol. 24, no. 3, pp. 264–268, Mar. 2017.
- [15] S. Zhang, B. Xiao, K. Xiao, Z. Chen, and B. Xia, "Design and analysis of irregular sparse code multiple access," in *Proc. WCSP*, Nanjing, China, Oct. 2015, pp. 1–5.
- [16] Y. Du, B. Dong, Z. Chen, J. Fang, and L. Yang, "Shuffled multiuser detection schemes for uplink sparse code multiple access systems," *IEEE Commun. Lett.*, vol. 20, no. 6, pp. 1231–1234, Jun. 2016.
- [17] B. Xiao, K. Xiao, S. Zhang, Z. Chen, B. Xia, and H. Liu, "Iterative detection and decoding for SCMA systems with LDPC codes," in *Proc. WCSP*, Nanjing, China, Oct. 2015, pp. 1–5.
- [18] F. Wei and W. Chen, "Low complexity iterative receiver design for sparse code multiple access," *IEEE Trans. Commun.*, vol. 65, no. 2, pp. 621–634, Feb. 2017.
- [19] J. Chen, Z. Zhang, S. He, J. Hu, and G. E. Sobelman, "Sparse code multiple access decoding based on a Monte Carlo Markov chain method," *IEEE Signal Process. Lett.*, vol. 23, no. 5, pp. 639–643, May 2016.
- [20] D. Cai, P. Fan, and P. T. Mathiopoulos, "A tight lower bound for the symbol error performance of the uplink sparse code multiple access," *IEEE Wireless Commun. Lett.*, vol. 6, no. 2, pp. 190–193, Apr. 2017.
- [21] J. Bao, Z. Ma, M. Xiao, Z. Ding, and Z. Zhu, "Performance analysis of uplink SCMA with receiver diversity and randomly deployed users," *IEEE Trans. Veh. Technol.*, vol. 67, no. 3, pp. 2792–2797, Mar. 2018.
- [22] P. Xu, Y. Yuan, Z. Ding, X. Dai, and R. Schober, "On the outage performance of non-orthogonal multiple access with 1-bit feedback," *IEEE Trans. Wireless Commun.*, vol. 15, no. 10, pp. 6716–6730, Oct. 2016.
- [23] D. N. Tse, "Optimal power allocation over parallel Gaussian broadcast channels," in *Proc. ISIT*, Ulm, Germany, Jun./Jul. 1997, p. 27.
- [24] X. Wang and N. Gao, "Stochastic resource allocation over fading multiple access and broadcast channels," *IEEE Trans. Inf. Theory*, vol. 56, no. 5, pp. 2382–2391, May 2010.
- [25] Z. Yang, X. Lei, Z. Ding, P. Fan, and G. K. Karagiannidis, "On the uplink sum rate of SCMA system with randomly deployed users," *IEEE Wireless Commun. Lett.*, vol. 6, no. 3, pp. 338–341, Jun. 2017.
- [26] M. Moltafet, N. M. Yamchi, M. R. Javan, and P. Azmi, "Comparison study between PD-NOMA and SCMA," *IEEE Trans. Veh. Technol.*, vol. 67, no. 2, pp. 1830–1834, Feb. 2018.
- [27] Y. Dai, M. Sheng, K. Zhao, L. Liu, J. Liu, and J. Li, "Interference-aware resource allocation for D2D underlaid cellular network using SCMA: A hypergraph approach," in *Proc. WCNC*, Doha, Qatar, Apr. 2016, pp. 1–6.
- [28] L. Li, Z. Ma, L. Wang, P. Z. Fan, and L. Hanzo, "Cutoff rate of sparse code multiple access in downlink broadcast channels," *IEEE Trans. Commun.*, vol. 65, no. 8, pp. 3328–3342, Aug. 2017.
- [29] T. M. Cover and J. A. Thomas, *Elements of Information Theory*. New York, NY, USA: Wiley, 1991.
- [30] L. Li, N. Jindal, and A. Goldsmith, "Outage capacities and optimal power allocation for fading multiple-access channels," *IEEE Trans. Inf. Theory*, vol. 51, no. 4, pp. 1326–1347, Apr. 2005.
- [31] M. Dabiri and H. Saeedi, "Dynamic SCMA codebook assignment methods: A comparative study," *IEEE Commun. Lett.*, vol. 22, no. 2, pp. 364–367, Feb. 2018.
- [32] H. Lütkepohl, *Handbook of Matrices*. Chichester, U.K.: Wiley, 1996.
- [33] L. Li and A. J. Goldsmith, "Capacity and optimal resource allocation for fading broadcast channels. II. Outage capacity," *IEEE Trans. Inf. Theory*, vol. 47, no. 3, pp. 1103–1127, Mar. 2001.
- [34] CVX: *Matlab Software for Disciplined Convex Programming. Version 2.0 Beta*, CVX Res. Inc., Stanford, CA, USA, Sep. 2012.
- [35] S. Boyd and L. Vandenberghe, *Convex Optimization*. Cambridge, U.K.: Cambridge Univ. Press, 2004.
- [36] V. Solo and X. Kong, *Adaptive Signal Processing Algorithms: Stability and Performance*. Englewood Cliffs, NJ, USA: Prentice-Hall, 1995.



Jiaxuan Chen received the B.S. degree from Tsinghua University, Beijing, China, in 2016, where she is currently pursuing the Ph.D. degree with the Department of Electronic Engineering.

Her current research interests include wireless communications, signal processing, and optical wireless communications.



Zhaocheng Wang (M'09–SM'11) received the B.S., M.S., and Ph.D. degrees from Tsinghua University in 1991, 1993 and 1996, respectively. From 1996 to 1997, he was a Post-Doctoral Fellow with Nanyang Technological University, Singapore. From 1997 to 1999, he was a Research Engineer/Senior Engineer with OKI Techno Centre Pte. Ltd., Singapore. From 1999 to 2009, he was a Senior Engineer/Principal Engineer with Sony Deutschland GmbH, Germany. Since 2009, he has been a Professor with the Department of Electronic Engineering, Tsinghua University,

where he is currently the Director of the Broadband Communication Key Laboratory, Beijing National Research Center for Information Science and Technology.

He holds 34 US/EU granted patents (23 of them as the first inventor) and published over 135 peer-reviewed international journal papers. He authored or co-authored two books, which have been selected by IEEE Series on Digital & Mobile Communication and published by Wiley-IEEE Press. His research interests include millimeter wave communications, optical wireless communications and digital broadcasting.

Dr. Wang is a Fellow of the Institution of Engineering and Technology. He received the ICC2013 Best Paper Award, the OECC2015 Best Student Paper Award, the 2016 IEEE Scott Helt Memorial Award, the 2016 National Award for Science and Technology Progress (First Prize) and the ICC2017 Best Paper Award. He was also technical program co-chairs of many international conferences including ICC and GlobeSIP. He was an Associate Editor of the IEEE TRANSACTIONS ON WIRELESS COMMUNICATIONS from 2011 to 2015 and the IEEE COMMUNICATIONS LETTERS from 2013 to 2016.



Wei Xiang (S'00–M'04–SM'10) received the B.Eng. and M.Eng. degrees in electronic engineering from the University of Electronic Science and Technology of China, Chengdu, China, in 1997 and 2000, respectively, and the Ph.D. degree in telecommunications engineering from the University of South Australia, Adelaide, Australia, in 2004.

From 2004 to 2015, he was with the School of Mechanical and Electrical Engineering, University of Southern Queensland, Toowoomba, Australia. He is currently the Founding Professor and the Head

of Discipline of Internet of Things Engineering with James Cook University, Cairns, Australia. He has published over 220 peer-reviewed papers with nearly 100 IEEE journal articles. His research interest falls under the broad areas of communications and information theory, particularly the Internet of Things, and coding and signal processing for multimedia communications systems. He is an elected Fellow of the IET and Engineers Australia. He was a recipient of the TNQ Innovation Award in 2016, and the Pearcey Entrepreneurship Award (Highly Commended) in 2017, and the Engineers Australia Cairns Engineer of the Year in 2017. He was a co-recipient of three Best Paper Awards at 2015 WCSP, 2011 IEEE WCNC, and 2009 ICWMC. He has been awarded several prestigious fellowship titles. He was named a Queensland International Fellow from 2010 to 2011 by the Queensland Government of Australia, an Endeavour Research Fellow from 2012 to 2013 by the Commonwealth Government of Australia, a Smart Futures Fellow from 2012 to 2015 by the Queensland Government of Australia, and the JSPS Invitational Fellow jointly by the Australian Academy of Science and Japanese Society for Promotion of Science from 2014 to 2015. He is the Vice Chair of the IEEE Northern Australia Section. He was an Editor of the IEEE COMMUNICATIONS LETTERS from 2015 to 2017. He is an Associate Editor for the Springer's *Telecommunications Systems*. He has severed in a large number of international conferences in the capacity of General Co-Chair, TPC Co-Chair, and Symposium Chair.



Sheng Chen (M'90–SM'97–F'08) received the B.Eng. degree in control engineering from the East China Petroleum Institute, Dongying, China, in 1982, the Ph.D. degree in control engineering from the City University, London, in 1986, the D.Sc. degree from the University of Southampton, Southampton, U.K., in 2005. From 1986 to 1999, He held research and academic appointments at the Universities of Sheffield, Edinburgh and Portsmouth, all in U.K. Since 1999, he has been with the School of Electronics and Computer Science,

University of Southampton, U.K., where he is currently a Professor in intelligent systems and signal processing. He has published over 600 research papers. His research interests include adaptive signal processing, wireless communications, modeling and identification of nonlinear systems, neural network and machine learning, intelligent control system design, and evolutionary computation methods and optimization. He is a Fellow of the United Kingdom Royal Academy of Engineering, a Fellow of IET, and a Distinguished Adjunct Professor with King Abdulaziz University, Jeddah, Saudi Arabia, and an ISI highly cited researcher in engineering in 2004.